Two-electron system in a Gaussian quantum dot in a Magnetic field

Thesis submitted in partial fulfillment of the

requirements for the award of the degree of

Master of Technology

in

Computational Techniques

by

PALAKOLANU RAMANA REDDY

School of Physics

University of Hyderabad

Hyderabad 500 046

India

November 2010

To

My Family & Friends

DECLARATION

I hereby declare that the work reported in this thesis has been carried out by me independently in the school of physics, University of Hyderabad, under the supervision of
Prof. Ashok Chatterjee, School of Physics, University of Hyderabad . I also declare that this is my own work and effort, and it has not been submitted at any other University or Institution for any degree. Wherever contributions of others are involved, every effort is made to indicate that clearly with due reference to literature, and acknowledgement of collaborative research and discussions.

Place:

Date: **Palakolanu Ramana Reddy**

CERTIFICATE

This is to certify that the project work entitled " **Two-electron system in a Gaussian quantum dot in a magnetic field**" being submitted to University of Hyderabad by **Palakolanu ramana Reddy** with Reg.No. **08PCMT08**, in partial fulfillment for the award of the degree of Master of Technology in Computational Techniques, is a bonafide work carried out by him under my supervision.

Dean
School of Physics,
University of Hyderabad.

Prof. Ashok Chatterjee
Project Supervisor,
School of Physics,
University of Hyderabad.

ACKNOWLEDGMENTS

This thesis is the result of work whereby I have been accompanied and supported by many people. It is a pleasant aspect that I have now the opportunity to express my gratitude for all of them.

With immense pleasure I express my sincere gratitude, regards and thanks to my supervisor **Prof. Ashok Chatterjee** for his excellent guidance, invaluable suggestions and continuous encouragement at all the stages of my research work. His interest and confidence in me was the reason for all the success I have made. I have been fortunate to have him as my guide as he has been a great influence on me, both as a person and as a professional..

I gratefully acknowledge **Prof. V. S. S. Sastry** and also thankful to **Prof. K.P.N. Murthy**, **Prof. S. Chaturvedi**, **Dr. Janaki Balakrishnan** and **Dr. Suneel Singh** for their valuable teaching during my M.Tech course.

I am extremely grateful to **The Dean**, school of physics, for providing excellent computing facilities and a nice atmosphere for doing my project.

I thank $Mr.T.Abraham$ for his help in administrative matters and $Mr.K.Srinivas$ for his help in lab related matters.

I would like to thank all my friends for their smiles and friendship making the life at UOH enjoyable and memorable.

Above all, I am blessed with such caring parents. I extend my deepest gratitude to my parents, my brother and sisters for their invaluable love, affection, encouragement and support.

Palakolanu ramana Reddy

SUMMARY

Interest in the subject of quantum dots has continued unabated for the last three decades. In the present thesis we shall investigate the effect of quantum confinement on the energy of a two-electron system in a quantum dot. We will be mainly interested in a GaAs quantum dot with Gaussian confinement.

In Chapter 1 we will present a general overview of the subject of quantum dots. We shall introduce three main types of low-dimensional systems such as quantum wells, quantum wires, and quantum dots and shall briefly describe some of their important properties as have been observed through experiments in the laboratory. In general, it has been observed that the electronic, optical, magnetic and thermal properties of quantum dots are size dependent and this behavior is generally known as the quantum size effect. We shall also show that the density of states behave differently as one goes on reducing the dimensionality of a system and this change in the density of states is really crucial for the difference in the behavior of the low-dimensional systems as compared to the bulk systems. We will present a discussion on micro-fabrication methods for preparing quantum dots in the laboratory and their relative advantages and disadvantages. Finally we will present some of the important applications of the quantum dots.

In Chapter 2 we will introduce the very important concept of charge quantization which hardly manifests itself in the case of bulk systems but plays a crucial in the low-dimensional systems. We shall also introduce the phenomenon of Coulomb blockade which has become a very important issue in quantum dot devices and elaborate the conditions under which it becomes experimentally relevant. We will also discuss briefly the concept of single electron transistors.

One of the important inputs that one would require to have in the case of theoretical studies of a quantum dot is the nature of the confinement potential. The simplest model for confinement may be simulated by an infinitely deep potential well. However it is a very unrealistic model.

In Chapter 3 we will show using the results of some cyclotron resonance experiments, and Kohn's theorem and generalized Kohn's theorem that the confining potential in a quantum dot is more or less periodic. After knowing the form of the confinement potential, one would like to

study the behavior several quantum mechanical systems in a parabolic quantum dot.

In Chapter 4 we will study the behaviour of the ground state energy of a system of two electrons in a two-dimensional parabolic quantum dot in the presence of an external magnetic field. We will investigate this problem using the WKB approximation method. Following the work of S.Klama[1] in excellent agreement with the exact numerical results. Also we shall extend the work to $3D$ spherical potential and study the effect of the size of the dot and the depth of the confinement potential on the energy of the two electron system.

Recent experiments have shown that the confinement potential in a quantum dot is not strictly parabolic, but rather it is anharmonic. In this context it has been reported in the literature that a Gaussian potential would be a better choice for the confinement potential. Several investigations have subsequently followed using the Gaussian confinement model for the quantum dot. In chapter 5 we will study the same problem of a system of two electrons in a quantum dot in a magnetic field using the Gaussian confinement. We shall also compare our results with the corresponding parabolic model. We shall study the problem in both two and three dimensions. We shall show that though for a large dot parabolic confinement model works fairly well, in the case of a small dot, the parabolic model is only a poor approximation of the more realistic Gaussian model.

Contents

1 Introduction **1**

1.1 Properties of Quantum dots 2

1.1.1 Density of states 2

1.1.2 Specific heat 3

1.1.3 Susceptibility 3

1.1.4 Blue shift: 3

1.1.5 Optical Properties 4

1.1.6 Electronic Properties 4

1.2 Methods of Preperation 5

1.2.1 Etching 5

1.2.2 Modulated electric field 6

1.2.3 Selective growth 8

1.3 Applications 8

1.3.1 Computing 9

1.3.2 Biology 9

1.3.3 Photovoltaic devices 10

1.3.4 Light emitting devices 10

2 Charge quantization and Coulomb blockade **12**

2.1 Charge Quantization 12
2.2 Coulomb Blockade in Nanocapacitor 14
2.2.1 Temperature effect in Coulomb Blockade 17
2.2.2 Heisenberg uncertainty relation 17
2.3 Coulomb Blockade in a Quantum Dot Circuit 18
2.4 Single Electron Devices 21
2.4.1 Advantages 22
2.4.2 Disadvantages 22

3 Confinement Potential 23
3.1 Cyclotron Resonance Experiments: 23
3.2 Kohn's Theorem 24
3.2.1 Proof of the theorem: 24
3.2.2 Generalized Kohn's Theorem 28
3.2.3 Proof of the theorem: 28

4 Two electron system in a parabolic quantum dot in a magnetic field 35
4.1 The Model 35
4.2 The transformation into a One-Body problem 36
4.3 WKB Method for 2D PQD 39
4.4 Results and Discussions 40

5 Two electron system in a gaussian quantum dot in a magnetic field 44
5.1 Introduction 44
5.2 The Model 45
5.3 Harmonic Approximation 45
5.3.1 The transformation into a One-Body problem 48
5.3.2 WKB Solution: 50

5.4 Results and Discussions: 51

6 Conclusion **57**

Chapter 1

Introduction

Semiconductor quantum dots are nano-scale materials in which the electron motion is confined in all the three directions. This leads to quantum size-effects to which the dot woes its name. The name quantum dot is relatively recent, but the effects of confinement have been manifested in many observations before. In the 1920's it was observed that heating glasses containing CdS colloids, shifts the onset of the absorption and the luminescence color to longer wavelengths. This was correctly correlated to the growth of CdS colloids upon heating .

In the 1960's, researchers reported differences between the absorption spectra of colloidal semiconductor particles and the spectra of the corresponding macroscopic material . The observed shift in the absorption curve was unclear and was attributed to distortions of the conduction and valence bands near the crystal surface, or to changes in the phonon spectrum caused by crystal boundaries . A major breakthrough took place at the end of 1960's, when the Molecular Beam Epitaxy (MBE) method was developed at the Bell Laboratories . Soon after the invention of MBE, the experimental observation of quantized energy levels of confined charge carriers was reported in 2D-structures . Subsequently, researchers tried to reduce the dimensions of these systems even further.

Quantum dots were discovered in the beginning of the 1980's by Alexei Ekimov in a glass matrix and by Louis E. Brus in colloidal solutions. The term "**Quantum Dot**" was coined by Mark

Reed.

1.1 Properties of Quantum dots

Because of the full confinement of carriers inside the dots, their properties drastically differ from those of bulk three dimensional (3D) materias. In these materials one can observe discrete quantum levels. Some of the versatile properties of quantum dots that opened doors to a new era in condensed matter physics are as follows.

1.1.1 Density of states

The discretization of the energy spectrum enhances the sharpness of the density of states. In Figure:1.1, the changes in the nature of the density of states with the corresponding reduction in the dimensionality are presented.

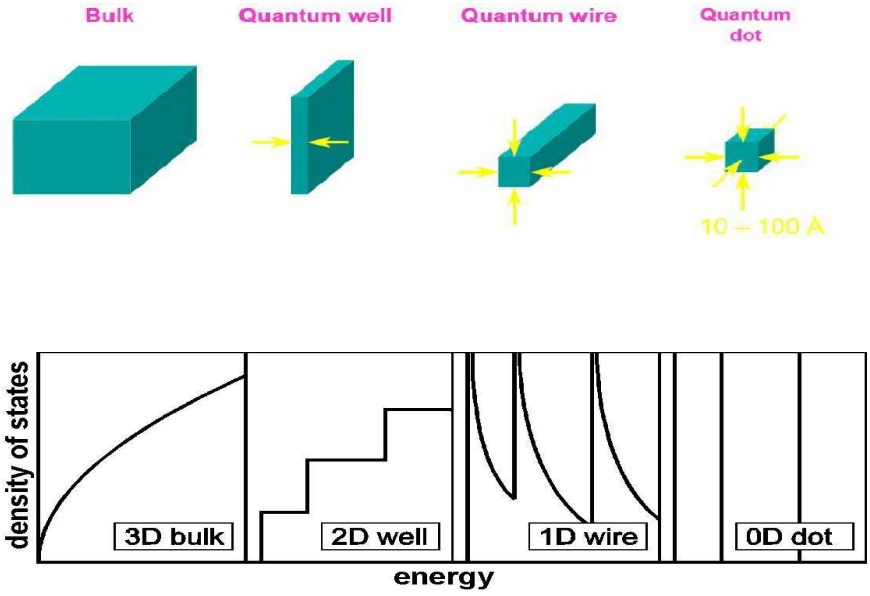

Figure 1.1: Density of states as a function of energy in systems with different spatial dimensionality. 3D refers to a bulk system, 2D refers to a quantum well, 1D corresponds to quantum wire and 0D represents a quantum dot.

The density of states is defined as $D(E) = \frac{dN}{dE}$ where N is the number of electrons having energy up to E. This means that the number of electrons dN lying within a narrow range of energy dE at E is proportional to the density of states at E. The density of states in a quantum dot is given by δ - function peaks.

1.1.2 Specific heat

At low temperature there is a siginificant contribution from the conduction electrons to the specific heat and this depends on the electronic density of states at the Fermi level. Since the electronic specific heat depends on the density of states which in turn depends on the dimensionality of the system, one would expect that the electronic specific heat will be different in a quantum dot as compared to its value in its bulk counterpart.

1.1.3 Susceptibility

The component of the susceptibility arising from the conduction electrons, called the Pauli susceptibility is directly proportional to the density of state

$$\chi_{pauli} = \mu_B^2 D(E_F) \tag{1.1}$$

where μ_B is the permeability of the material.

Thus it is clear that that Pauli susceptibility will have a different behaviour in a quantum dot.

1.1.4 Blue shift:

The band-gap in a quantum dot will always be energetically larger; therefore, we refer to the radiation from quantum dots to be blue shifted reflecting the fact that electrons must fall a greater distance in terms of energy and thus produce radiation of a shorter, and therefore bluer wave-

length. The quantum Dot allows us to control its band gap by adjusting its size and hence helps in controlling the output wavelength with extreme precision.

1.1.5 Optical Properties

An immediate optical feature of colloidal quantum dots is their coloration. While the material which makes up a quantum dot defines its intrinsic energy signature, the nanocrystal's quantum confined size is more significant at energies near the band gap. Thus quantum dots of the same material, but with different sizes, can emit light of different colors. The physical reason is the quantum confinement effect.

The larger the dot, the redder (lower energy) its fluorescence spectrum. Conversely, smaller dots emit bluer (higher energy) light. The coloration is directly related to the energy levels of the quantum dot. Quantitatively speaking, the band-gap energy that determines the energy (and hence color) of the fluorescent light is inversely proportional to the size of the quantum dot. Larger quantum dots have more energy levels which are also more closely spaced. This allows the quantum dot to absorb photons containing less energy, i.e., those closer to the red end of the spectrum.

1.1.6 Electronic Properties

At sufficiently low temperatures the energy of the phonons is too low to excite the electrons in QD and the strong quantization of energy determines the electronic properties these systems. In addition to affecting the electronic structure of quantum dots, quantum confinement has consequences for the quantum dot charging and charge transport. Some relevant electronic properties that are size dependent are the polarization energy, the Coulomb charging energy and the optical excitation energy.

1.2 Methods of Preperation

Unlike quantum wells, where the motion of carriers is restricted to a plane through the crystallization of thin epitaxial layers, the creation of quantum wires or dots, which confine the carriers in a space with at least two of the three dimensions limited to the range of the de Broglie wavelength, requires far more advanced technology.

1.2.1 Etching

The earliest method of manufacturing quantum dots was implemented by Reed et al [2] , who etched them in a structure containing a two-dimensional electron gas. Subsequent steps of this process are shown in Figure:1.2(a).

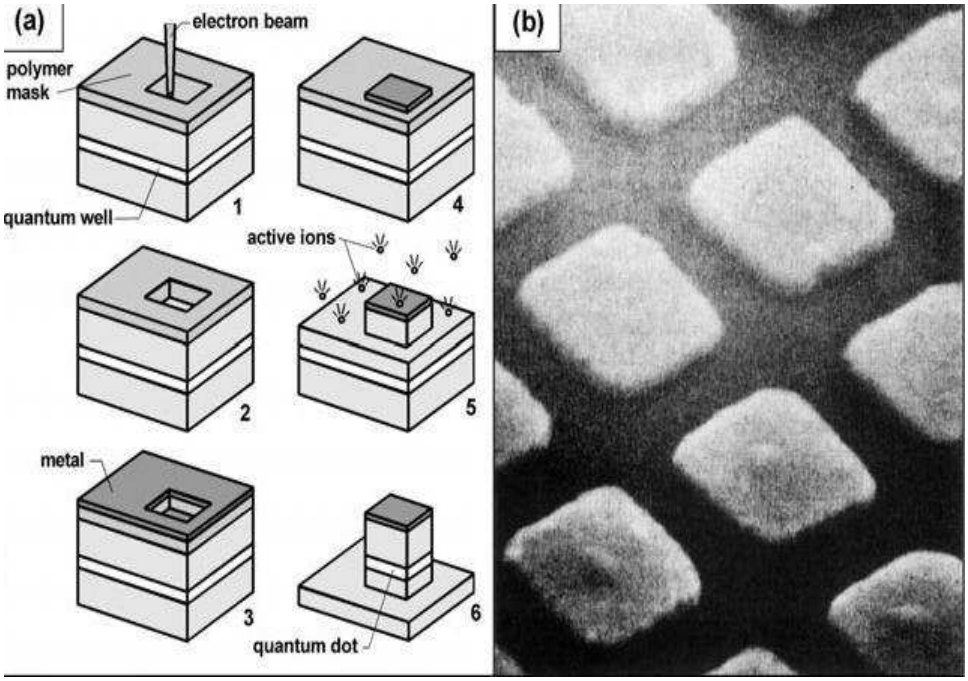

Figure 1.2: (a) Process of quantum dot etching .(b) Etched quantum dots in a GaAs/AlGaAs well, electron scanning microscope picture.

1. The surface of a sample containing one or more quantum wells is covered with a polymer mask, and then partly exposed.

2. The exposed pattern corresponds to the shape of the created nanostructure. Owing to the required high resolution, the mask is not exposed to visible light, but to the electron or ion beam (electron/ion-beam lithography). In the exposed areas the mask is removed.

3. Later, the entire surface is covered with a thin metal layer.

4. Using a special solution, the polymer film and the protective metal layer are removed, and a clean surface of the sample is obtained, except for the previously exposed areas, where the metal layer remains.

5. Next the areas not protected by the metal mask are chemically etched.

6. Slim pillars are created, containing the cut-out fragments of quantum wells.

In this way, the motion of electrons, which is initially confined in the plane of the quantum well, is further restricted to a small pillar with a diameter of the order of $10 - 100nm$. Owing to the simplicity of the production of thin, homogeneous quantum wells, GaAs is the most commonly used material for creating dots by means of etching. Fig:1.2(b)presents a picture of real dots obtained using this method.

1.2.2 Modulated electric field

Another method involves the creation of small electrodes over the surface of a quantum well by means of lithographic techniques. Application of an appropriate voltage to the electrodes produces a spatially modulated electric field, which localizes the electrons within a small area. The lateral confinement created in this way has no edge defects, which are characteristic of etched structures. The process of spreading a thin electrode over the surface of a quantum well may produce both single quantum dots [3] and large arrays (matrices) of dots [4, 5].

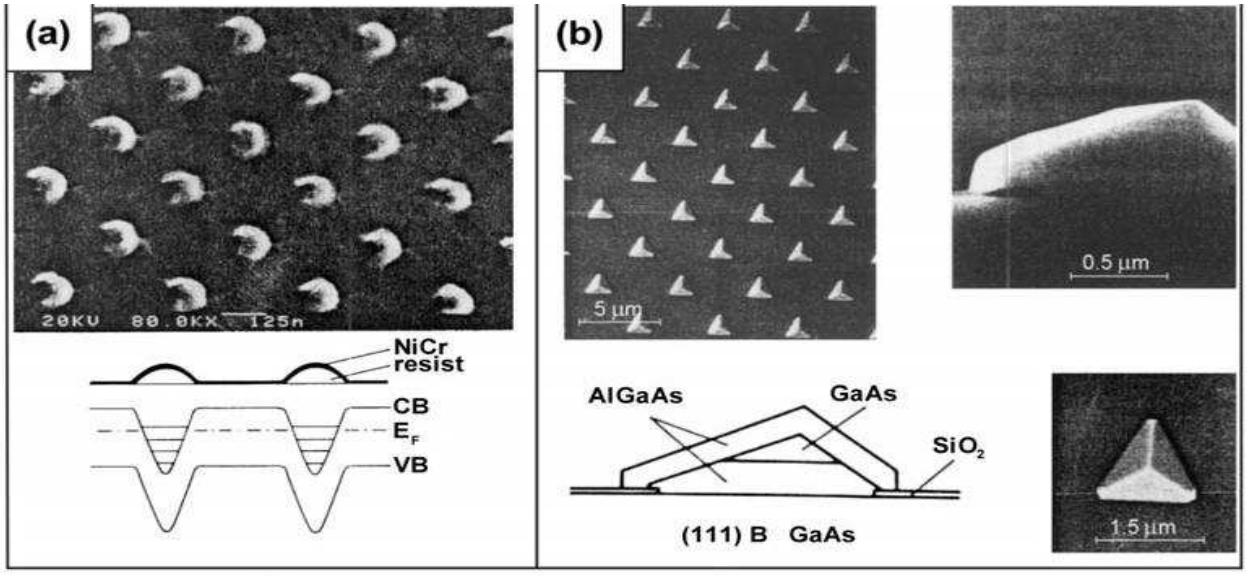

Figure 1.3: (a) Quantum dots produced on InSb in which the electrons are confined by the electric field (electron scanning microscope picture). Bottom: Shape of the electrode and the configuration of band edges (valence and conduction bands). (b) Quantum dots created on the surface of GaAs in the selective Metal-Organic Chemical Vapour Deposition (MOCVD) growth (scanning electron microscope pictures). The configuration of layers in a single dot is shown. The width of the electron localization area at the top of the pyramid of the order of $100nm$.

Modulation of the electric potential, produced by applying a voltage to an electrode, can be realized by the previous preparation (using a lithographic technique) of a regular array of islets of non-metallic material (e.g. of the barrier material) on the surface of the sample. As a result, the distance between the electrode (overlaying the surface with the islets) and the plane of the quantum well is modulated, and the electrons are bound in small areas under the prepared islets. A photograph of a matrix of such dots, together with the profile of the confining potential, is shown in Figure:1.3(a).Instead of modulating the distance between the electrode and the well, it is also possible to build a pair of parallel, thin electrodes above the well. The lower one can have regularly placed holes which is where quantum dots are to be created .

A voltage applied to the pair of electrodes results in a change in both the dot size and the depth of the confining potential. The potential depth influences the number of confined electrons. However, when an additional electrode is introduced between the quantum-well layer and the

doped layer, the number of electrons and the potential depth can be changed independently. Even more complicated systems of micro-electrodes are applied now a days [6].

1.2.3 Selective growth

The next method is the selective growth of a semiconducting compound with a narrower band gap (e.g. $GaAs$) on the surface of another compound with a wider band gap (e.g. $AlGaAs$) [7] . Restriction of growth to chosen areas is obtained by covering the surface of the sample with a mask (SiO2) and etching miniature triangles on it. On the surface not covered by the mask the growth is then carried out with the metal-organic chemical vapour deposition method $(MOCVD)$, at a temperature of $700 - 800°C$. The crystals created have the shape of tetrahedral pyramids. The first crystallized layers are the layers of the substrate compound $(AlGaAs)$, and only the top of the pyramid is created of GaAs. Thus it is possible to obtain a dot with an effective size under $100nm$. Pictures of such dots, and the configuration of GaAs/AlGaAs layers, are shown in fig:1.3(b).

1.3 Applications

Quantum dots are particularly significant for optical applications due to their high extinction co-efficient [8] . In electronic applications they have been proven to operate like a single-electron transistor and show the Coulomb blockade effect. Quantum dots have also been suggested as implementations of qubits for quantum information processing.

The ability to tune the size of quantum dots is advantageous for many applications. For instance, larger quantum dots have a greater spectrum-shift towards red compared to smaller dots, and exhibit less pronounced quantum properties. Conversely, the smaller particles allow one to take advantage of more subtle quantum effects.

Being zero dimensional, quantum dots have a sharper density of states than higher-dimensional structures. As a result, they have superior transport and optical properties, and are being researched

for use in diode lasers, amplifiers, and biological sensors. Quantum dots may be excited within the locally enhanced electromagnetic field produced by the gold nanoparticles, which can then be observed from the surface Plasmon resonance in the photoluminescent excitation spectrum of (CdSe)ZnS nanocrystals. High-quality quantum dots are well suited for optical encoding and multiplexing applications due to their broad excitation profiles and narrow/symmetric emission spectra. The new generations of quantum dots have far-reaching potential for the study of intracellular processes at the single-molecule level, high-resolution cellular imaging, long-term in-vivo observation of cell trafficking, tumor targeting, and diagnostics.

1.3.1 Computing

Quantum dot technology is one of the most promising candidates for use in solid-state quantum computation. By applying small voltages to the leads, the flow of electrons through the quantum dot can be controlled and thereby precise measurements of the spin and other properties therein can be made. With several entangled quantum dots, or qubits, plus a way of performing operations, quantum calculations and the computers that would perform them might be possible.

1.3.2 Biology

In modern biological analysis, various kinds of organic dyes are used. However, with each passing year, more flexibility is being required of these dyes, and the traditional dyes are often unable to meet the expectations. To this end, quantum dots have quickly filled in the role, being found to be superior to traditional organic dyes on several counts, one of the most immediately obvious being brightness (owing to the high extinction co-efficient combined with a comparable quantum yield to fluorescent dyes [9]) as well as their stability (allowing much less photobleaching). It has been estimated that quantum dots are 20 times brighter and 100 times more stable than traditional fluorescent reporters. For single-particle tracking, the irregular blinking of quantum dots is a minor drawback. The improved photostability of quantum dots, for example, allows the ac-

quisition of many consecutive focal-plane images that can be reconstructed into a high-resolution three-dimensional image. Researchers were able to observe quantum dots in lymph nodes of mice for more than 4 months.[10]

Semiconductor quantum dots have also been employed for in-vitro imaging of pre-labeled cells. The ability to image single-cell migration in real time is expected to be important to several research areas such as embryogenesis, cancer metastasis, stem-cell therapeutics, and lymphocyte immunology.

1.3.3 Photovoltaic devices

Quantum dots may be able to increase the efficiency and reduce the cost of today's typical silicon photovoltaic cells. According to an experimental proof, quantum dots of lead selenide can produce as many as seven excitons from one high energy photon of sunlight (7.8 times the bandgap energy). This compares favourably to today's photovoltaic cells which can only manage one exciton per high-energy photon, with high kinetic energy carriers losing their energy as heat. This would not result in a 7-fold increase in final output however, but could boost the maximum theoretical efficiency from 31% to 42%. Quantum dot photovoltaic cell would theoretically be cheaper to manufacture, as they can be made "using simple chemical reactions." The generation of more than one exciton by a single photon is called multiple exciton generation (MEG) or carrier multiplication.

1.3.4 Light emitting devices

There are several inquiries into using quantum dots as light-emitting diodes (LED) to make displays and other light sources, such as Quantum dot LED "$QD-LED$" displays, and "QD-WLED" (White LED). In June, 2006, QD Vision announced technical success in making a proof-of-concept quantum dot display and showed a bright emission in the visible and near infra-red region of the spectrum. Quantum dots are valued for displays, because they emit light in very specific gaussian

distributions. This can result in a display that more accurately renders the colors that the human eye can perceive. Quantum dots also require very little power since they are not color filtered. Additionally, since the discovery of ”white-light emitting” QD, general solid-state lighting applications appear closer than ever. A color liquid crystal display (LCD), for example, is usually powered by a single fluorescent lamp (or occasionally, conventional white LEDs) that is color filtered to produce red, green, and blue pixels. Displays that intrinsically produce monochromatic light can be more efficient, since more of the light produced reaches the eye.

Chapter 2

Charge quantization and Coulomb blockade

2.1 Charge Quantization

There are two kinds of charge, positive and negative. Like charges repel, unlike charges attract. Positive charge comes from having more protons than electrons; negative charge comes from having more electrons than protons. Charge is quantized, meaning that charge comes in integer multiples of the elementary charge e.

Probably everyone is familiar with the first three concepts, but what does it mean for charge to be quantized? Charge comes in multiples of an indivisible unit of charge, represented by e which has the magnitude $1.6 \times 10^{-19}C$. In other words, charge comes in multiples of the charge of the electron or the proton. A proton has a charge of $+e$, while an electron has a charge of $-e$. Charge quantization is a natural phenomenon, but it is hardly observable at the lab scale. Thus it does not have much significance for bulk materials. One example will clarify this point.

Consider an electric bulb of voltage $230V$, with power $60W$. Then the flow of charge per second is given by

$$I = \frac{powerA}{voltageV} = \frac{60A/s}{230V} = 0.2c/s. \tag{2.1}$$

Then the flow of electrons per second is of the order of 10^{18} electrons/sec. This rate is similar to that of a usual fluid flow. Therefore the charge quantization does not manifest itself in a bulk case. However in the case of a nanosystem, for example, in a quantum dot, the rate of electron flow is only a few electrons per second. So charge quantization really becomes observable in a nanomaterial.

Moreover in case of nanosystems, addition or subtraction of a few number of charge carriers (electrons) causes observable change in the energy. Consider a spherical capacitor with charge Q and capacitance C. The energy of the capacitor is given by

$$E = \frac{Q^2}{2C}. \tag{2.2}$$

On adding one electron,the energy of the capacitor becomes

$$E_1 = \frac{(Q+e)^2}{2C}. \tag{2.3}$$

If the radius of the capacitor is R, the capacitance in CGS units will be R. So we can write

$$E = \frac{Q^2}{2R}. \tag{2.4}$$

and

$$E_1 = \frac{(Q+e)^2}{2R}. \tag{2.5}$$

Thus, the change in the energy of the quantum dot will be

$$\triangle E \approx \frac{Qe}{R}. \tag{2.6}$$

and the relative change in energy is given by

$$\frac{\triangle E}{E} \approx \frac{e}{Q}. \tag{2.7}$$

For bulk systems the number of electrons is very high, so the relative energy is approximately zero. In the case of nanosystems the relative energy is nearly unity. So the change in energy of a quantum dot due to the addition of a single electron is of the same order as the energy of the dot itself. Thus the effect of a single electron can be observable in the case of a quantum dot and so the charge quantization becomes apparent in a quantum dot. Since $Q = n(-e)$, energy can be written as,

$$E = \frac{n^2 e^2}{2C}. \tag{2.8}$$

therefore the Hamiltonian can be written as

$$H = \frac{e^2}{2C}\vec{n}^2. \tag{2.9}$$

where n is the number operator. The Hamiltonian H commutes with n i.e.$[n, H] = 0$. Therefore we cannot have transport in such systems. We must have a tunneling factor in Hamiltonian and then transport occurs through the system.

2.2 Coulomb Blockade in Nanocapacitor

When a single electron tunnels through the insulating layer from the negative plate to the positive plate of a tunnel capacitor, it results in a decrease in the positive charge on the top plate,

$$Q \to Q + e = Q - |e| \tag{2.10}$$

and an increase in the positive charge on the bottom plate,

$$-Q \rightarrow -Q - e = -Q + |e| \tag{2.11}$$

The change in energy stored is

$$\triangle E = E^i - E^f = \frac{-e(Q + \frac{e}{2})}{C}. \tag{2.12}$$

It must be energetically favorable for the tunneling event to occur , and if we require $\triangle E > 0$, we find that

$$Q > \frac{-e}{2} \tag{2.13}$$

for tunneling to occur. In terms of the condition on voltage for the capaciter, we have

$$V > \frac{-e}{2C} \tag{2.14}$$

or,

$$V > \frac{|e|}{2C} \tag{2.15}$$

Energy is conserved , and since the stored energy decreases upon tunneling, the electron is excited above the Fermi level resulting in an increase in kinetic energy on the other side of the junction. So upon tunneling, the voltage over the junction will decrease by $\frac{|e|}{C}$ so that

$$V^i = \frac{Q}{C} = \frac{-e}{2C} \qquad \text{and} \qquad V^f = \frac{Q - |e|}{C} = -\frac{|e|}{2C}. \tag{2.16}$$

Repeating for opposite polarity, we find that in order for tunneling to occur, we must have

$$\frac{|e|}{2C} < V < -\frac{|e|}{2C}. \tag{2.17}$$

. Thus, tunneling current will only flow when a sufficiently large voltage($|V| > \frac{q_e}{2C}$) exists across the capacitor. This effect is called ***The Coulomb Blockade***. So there should be some minimum voltage called the threshold voltage for the tunneling and the corresponding energy

$$E_c = \frac{e^2}{2C} \tag{2.18}$$

is called the **charging energy of the capacitor**. This is the energy required to add an electron to the capacitor. This is because of the repulsion from the electron which already exists. For a macroscopic capacitor where $C = 1.1 * 10^{-13}$F, we need only $|V| > 0.73\mu V$ for tunneling to occur. So we can't observe Coulomb blockade in macroscopic capacitor. But for a nanocapacitor with $C = 1.1 * 10^{-19}F$, $|V| > 0.73V$ is required. Thus, Coulomb blockade is not evident in macro-sized circuits, but will be observed in nanometer scale circuits.

The I-V characteristics in a macro and nano capacitors at T=0K are shown in Figure:2.1.

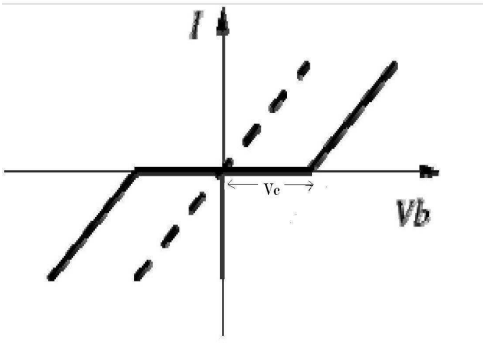

Figure 2.1: $I - V$ characteristics of nano and macro capacitors at $T = 0K$ .Dashed curve represents the macro capacitor and the solid curve represents the nanoscale capacitor.

2.2.1 Temperature effect in Coulomb Blockade

Temperature plays an important role in Coulomb blockade phenomenon. The preceding development is only strictly valid at T=0K. To observe the Coulomb blockade the charging energy in Eq.(2.18) should be larger than the thermal energy i.e.,

$$\frac{e^2}{2C} >> \frac{1}{2}k_B T, \tag{2.19}$$

or

$$T << \frac{e^2}{k_B C}, \tag{2.20}$$

where k_B is the Boltzmann's constant. For the nanoscale capacitor $(C = 1.1 * 10^{-19})$, $T << 16.19K$, which is obviously the typical situation. Therefore , we should be able to observe coulomb blockade for this capacitor in the laboratory. However , for the macro capacitor ($C = 1.1*10^{-13}F$), $T << 0.017K$, which may be difficult to achieve.

2.2.2 Heisenberg uncertainty relation

From uncertainty principle between energy and time

$$\triangle E \triangle t \geq \frac{\hbar}{2}. \tag{2.21}$$

The time constant for an RC ciruit is given by

$$\tau = R_t C. \tag{2.22}$$

τ is the characteristic time associated with tunneling events. This is not the time to tunnel through the junction, but, rather, the time between two tunneling events i.e., τ is considered to be the

approximate lifetime of the energy state of the electron on one side of the barrier. Thus, we have an uncertainty in the energy value given by

$$\triangle E \geq \frac{\hbar}{2R_t C}. \tag{2.23}$$

To observe the Coulomb blockade effect, the charging energy must be much larger than the uncertainty ΔE, this yiels

$$R_t > \frac{\hbar}{e^2} \simeq 4.1K\Omega. \tag{2.24}$$

Thus the tunneling resistance of the capacitor circuit must be larger than $4.1K\Omega$.

2.3 Coulomb Blockade in a Quantum Dot Circuit

If we place a quantum dot in between two leads , the transport of charge occurs due to tunneling i.e., current can flow from lead to lead through the quantum dot. In this type of situation the quantum dot which is merely a very small material region , is also called a quantum island or a coulomb island. The following figure represents the quantum island connected to the external

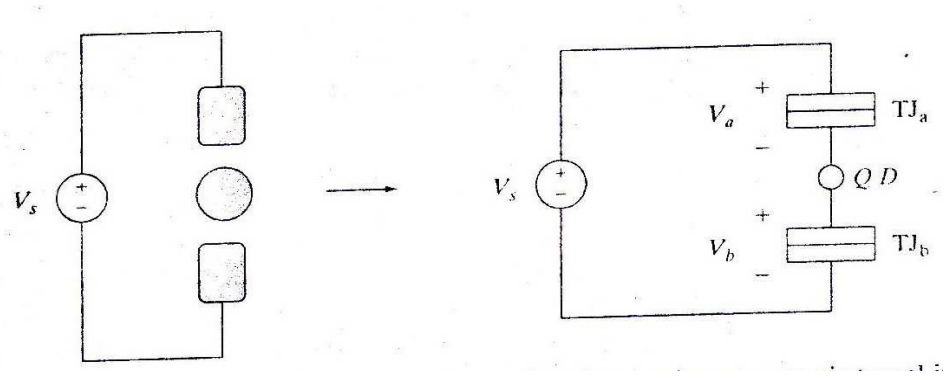

Figure 2.2: Equivalent circuit of a quantum dot connected to a voltage source via tunnel junctions

voltage source V_s , and its equivalent circuit. In this figure the tunnel junctions represent the

insulating regions isolating the island(dot) from the leads connected to an external source V_s. The tunnel junctions can be modeled by leaky capacitors. Therefore, for one junction we have C_a, and R_{ta}, and for the other junction,C_b, R_{tb}, where R_{ti} is the tunneling resistance of junction i. Associated with each tunnel junction , we have

$$Q = Q_b - Q_a. \tag{2.25}$$

Electron tunneling allows a discrete number of electrons to accumulate in the island, and so

$$Q = ne \tag{2.26}$$

where n is an integer. Assume that initially there are n electrons in the island. Let one electron tunnel onto the island through junction b.
This tunneling occurs when

$$V_s > \frac{-e}{C_a}(n + \frac{1}{2}). \tag{2.27}$$

In a similar manner, an electron tunnels form the island through junction a if

$$V_s > \frac{e}{C_a}(n - \frac{1}{2}). \tag{2.28}$$

As a special case , if we let $C_a = C_b = C$ and $n = 0$, then (2.27) and (2.28) both reduce to

$$V_s > \frac{-e}{2C}. \tag{2.29}$$

Now consider the opposite situation, where an electron tunnels on to the island through junction a , and off the island through junction b. For $C_a = C_b = C$ and $n = 0$, we would find

$$V_s < \frac{e}{2C} \tag{2.30}$$

Thus, under these conditions, we have

$$\frac{-e}{2C} < V_s < \frac{e}{2C} \tag{2.31}$$

or

$$|V_s| > \frac{e}{2C} \tag{2.32}$$

i.e., the same Coulomb blockade as encountered for the single capacitor .

Now assume that one electron has already tunneled onto the island through junction b. If a second electron tunnels onto the dot through junction b, we would find that

$$V_s > \frac{-e}{C_a}(n + \frac{3}{2}). \tag{2.33}$$

For the case $C_a = C_b = C$ and $n = 0$, and considering different tunneling directions , we obtain

$$|V_s| > \frac{3|e|}{2C}. \tag{2.34}$$

Considering a third tunneling event, we would obtain

$$|V_s| > \frac{5|q_e|}{2C}, \tag{2.35}$$

and, in general, we have

$$|V_s| > \frac{me}{2C}. \tag{2.36}$$

where $m = 1, 3, 5, \ldots$, for $1, 2, 3 \ldots$ electron tunneling events respectively. Thus, electron tunneling, giving rise to currents, will occur at discrete voltage steps. The resulting $I - V$ Characteristic curve, known as the ***Coulomb staircase*** , is depicted in the figure below. where $V_1 = e/2C$, and $I_1 = e/R_t C_s$.

2.4 Single Electron Devices

The term single electron devices in fact , is a bit of a misnomer, and in literature, the term "single-electron precision" device has been suggested as a more descriptive name. This is due to the fact that usually much more than one electron is involved, although the number may be relatively small. It is important to note that these devices are typically sensitive to the transfer of single electronic charge and therefore they can operate by manipulating an extremely small number of electrons.

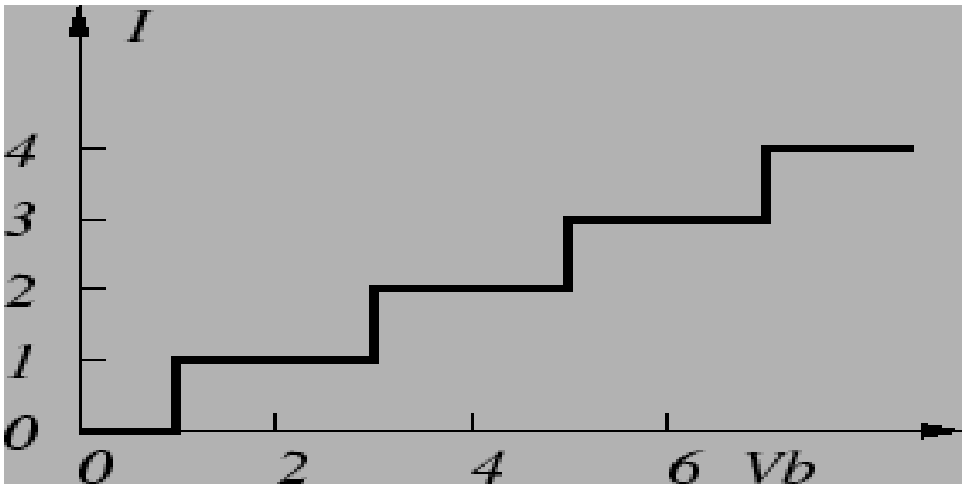

Figure 2.3: Coulomb stair case in a double junction system

2.4.1 Advantages

1. They offer potential benefits of ultra large scale integration with devices which have dimensions of the order of nanometers.

2. They also exhibit very low power dissipation and high speed.

2.4.2 Disadvantages

1. If a device is sensitive to the movement of a single electronic charge, then the presence of a single charge impurity, may drastically influence the device operation.

2. Device fabrication is very difficult.

Chapter 3

Confinement Potential

In quantum dots one of the challenging issues is to find the nature of the attractive confining potential for the electrons in the quantum dot. In general the simplest way to describe a quantum dot is to consider the model of an electron confined in an infinite potential well. But the force experienced by the electron according to such a model is zero in the quantum dot and so this model of potential is not correct.

3.1 Cyclotron Resonance Experiments:

Sirkosky and Merkt [13] have found experimentally that the resonance frequency in a quantum dot does not depend on the number of electrons in the dot. The independence of the excitation energy on the number of electrons indicates that the excitation spectrum of a quantum dot is not influenced by the electron-electron interaction. This is in contrast to the situation in real atoms. Later, Meurer et al. [14] have studied the few-electron quantum dot energy using the far infrared spectroscopy on GaAs quantum dot and have observed that resonance frequency has only a weak dependence on the electron number. Independence of the dipole transitions on the electron number

was also approximately observed in GaAs- GaAlAs quantum dots by Ashoori [15] and in the InGaAs-GaAs-AlAs system by Drexler [16]. All these results suggest an interesting feature about the quantum dot which is reminiscent of the celebrated Kohn theorem.

3.2 Kohn's Theorem

Kohn's theorem states that " For an electron gas placed in an external magnetic field, the cyclotron frequency is independent of the electron-electron interaction". This theorem is a consequence of the fact that the electric dipole of the radiation field couples only to the centre of mass of the electrons and does not affect the relative motion.

3.2.1 Proof of the theorem:

The Hamiltonian of an interacting many electron system of N electrons is given by

$$H = \frac{1}{2m}\sum_{i=1}^{N} p_i^2 + \frac{1}{2}\sum_{i,j=1,i\neq j}^{N} U(|\vec{r_i} - \vec{r_j}|). \tag{3.1}$$

Here $\vec{p_i}$ is the momentum operator for the i^{th} electron, m its mass and $U(|\vec{r_i}-\vec{r_j}|)$ is the potential due to the electron-electron interaction. In the presence of a magnetic field B, $\vec{p_i}$ is replaced by $(\vec{p_i} - \frac{e\vec{A_i}}{c})$, where $\vec{A_i}$ is the vector potential satisfying the condition $\vec{\bigtriangledown} \times \vec{A} = \vec{B}$. So the Hamiltonian changes to

$$H = \frac{1}{2}\sum_{i=1}^{N} (\vec{p_i} - \frac{e\vec{A_i}}{c})^{2} + \frac{1}{2}\sum_{i=j=1,i\neq j}^{N} U(|\vec{r_i} - \vec{r_j}|). \tag{3.2}$$

The equation of motion in the Heisenberg picture is given by

$$\frac{d\mathbf{P}}{dt} = \frac{1}{i\hbar}[\mathbf{P}, H]. \tag{3.3}$$

The Lorentz force is given by

$$\mathbf{F} = -\frac{e}{c}(\mathbf{v} \times \mathbf{B}) = -\frac{e}{mc}(\mathbf{P} \times \mathbf{B}), \tag{3.4}$$

where **B** is the uniform magnetic field in the z direction. From Eqns.(3.3) and (3.4) we get

$$\mathbf{F} = -\frac{e}{mc}(\mathbf{P} \times \mathbf{B}) = \frac{1}{i\hbar}[\mathbf{P}, H], \tag{3.5}$$

where $\vec{P}$ is the new momentum given by

$$\mathbf{P} = \sum_{i=1}^{N} \mathbf{P}_i, \tag{3.6}$$

with

$$\mathbf{P}_i = (\mathrm{p}_{ix}, \mathrm{p}_{iy} - \frac{eBx_i}{c}, \mathrm{p}_{iz}) = (P_{xj}, P_{yj}, P_{zk}). \tag{3.7}$$

We choose the Landau gauge for the vector potential i.e., $A(0, Bx, 0)$. From Eqn .(3.5), we get

$$\sum_{i=1}^{N}(\mathbf{P_i} \times \mathbf{B}) = \frac{1}{i\hbar}[\mathbf{P}, H], \tag{3.8}$$

Construct ladder operators as follows.

$$P_{\pm} = (P_x \pm iP_y). \tag{3.9}$$

Then we can write

$$[P_{\pm}, H] = [P_x \pm iP_y, H] = [P_x, H] \pm i[P_y, H]. \tag{3.10}$$

Also, we have

$$\frac{d\mathbf{P}}{dt} = \frac{d}{dt}(\mathbf{i}P_x + \mathbf{j}P_y + \mathbf{k}P_z). \tag{3.11}$$

For the x component, $(\frac{d\vec{P}}{dt})_x = \frac{dP_x}{dt}$, so that we have

$$\frac{1}{i\hbar}[P_x, H] = -\frac{e}{mc}(\mathbf{P} \times \mathbf{B})_x. \tag{3.12}$$

Therefore

$$[P_+, H] = [P_x \pm iP_y, H] = [P_x, H] + i[P_y, H], = i\hbar(-\frac{e}{mc}(\mathbf{P} \times \mathbf{B})_x - \frac{e}{mc}(\mathbf{P} \times \mathbf{B})_y), \tag{3.13}$$

which reduces to

$$[P_+, H] = i\hbar\left(-\frac{e}{mc}(P_yB) + \frac{ie}{mc}(P_xB)\right). \tag{3.14}$$

Thus we have

$$[P_+, H] = -\frac{eB\hbar}{mc}P_+. \tag{3.15}$$

Since the cyclotron frequency is given by

$$\omega_c = \frac{eB}{mc}, \tag{3.16}$$

$$[P_+, H] = -\hbar\omega_c P_+. \tag{3.17}$$

Similarly we can show that

$$[P_-, H] = \hbar\omega_c P_-. \tag{3.18}$$

So that we can write

$$[H, P_+] = \hbar\omega_c P_+, \tag{3.19}$$

and

$$[H, P_-] = -\hbar\omega_c P_-. \tag{3.20}$$

Let us consider the ground state wave function Ψ_o so that we have

$$H\Psi_0 = E\Psi_0. \tag{3.21}$$

From Eq.(3.19) and Eq.(3.20) we have

$$[H, P_+] = (HP_+ - P_+H) = \hbar\omega_c P_+,$$

$$HP_+ = P_+H + \hbar\omega_c P_+,$$

So, we get

$$(HP_+)\Psi_o = (P_+H)\Psi_o + (\hbar\omega_c P_+)\Psi_o,$$

$$H(P_+\Psi_o) = (E_o + \hbar\omega_c)(P_+\Psi_o). \tag{3.22}$$

Therefore we can say that if Ψ_0 is an eigenstate of H with energy E_0, then $P_+\Psi_0$ is also an eigenstate of H belonging to the energy $(E + \hbar\omega_c)$. This means that the first excited level is greater than the ground state energy by $\hbar\omega_c$ and in fact the energy levels are equidistant with the energy separation equal to $\hbar\omega_c$.

We can therefore conclude that the excitation spectrum of an interacting electron system consists of equi - distant energy levels with separation energy $\hbar\omega_c$. So the electron - electron interaction

does not alter the separation between the energy levels.

3.2.2 Generalized Kohn's Theorem

This theorem states that "The cyclotron frequency of the a system of electrons in a magnetic field and confined by a parabolic potential is also independent of the electron - electron interaction".

3.2.3 Proof of the theorem:

Let us first consider a system of N non - interacting electrons placed in two dimensions and confined by a parabolic potential. The Hamiltonian is given by

$$H_0 = \frac{1}{2m}\sum_{j=1}^{N}\vec{p_j}^2 + \frac{1}{2}m\omega^2\sum_{j=1}^{N}\vec{r_j}^2, \tag{3.23}$$

where $\vec{p_j} = (p_{xj}, p_{yj}, p_{zj})$.

Let us define dimensionless variables

$$\vec{\pi}_j = \frac{\vec{p_j}}{\sqrt{m\omega\hbar}}.$$

$$\vec{q_j} = \vec{r_j}\sqrt{\frac{m\omega}{\hbar}}. \tag{3.24}$$

The Hamiltonian then simplifies to

$$H_0 = \frac{\hbar\omega}{2}\sum_{j=1}^{N}(\vec{\pi}_j^2 + \vec{q}_j^2) \tag{3.25}$$

$$= \frac{\hbar\omega}{2}\sum_{k=x,y}\sum_{j=1}^{N}(\pi_{jk}^2 + q_{jk}^2), \tag{3.26}$$

where

$$\vec{\pi}_j^2 = \sum_{k=x,y}\pi_{jk}^2, \qquad\qquad \vec{q}_j^2 = \sum_{k=x,y} q_{jk}^2. \tag{3.27}$$

One can easily see that

$$[q_{jk}, \pi_{jk}] = \sqrt{\frac{m\omega}{\hbar m\omega\hbar}}[r_{jk}, P_{jk}] = \frac{1}{\hbar}i\hbar = i. \tag{3.28}$$

Let us now introduce the following operators:

$$a_{jk} = \frac{1}{\sqrt{2}}(q_{jk} + i\pi_{jk}) = \sqrt{\frac{m\omega}{2\hbar}}(r_{jk} + i\frac{P_{jk}}{m\omega}),$$

$$a_{jk}^{+} = \frac{1}{\sqrt{2}}(q_{jk}^{+} - i\pi_{jk}^{+}) = \sqrt{\frac{m\omega}{2\hbar}}(r_{jk} - i\frac{P_{jk}}{m\omega}), \tag{3.29}$$

which obey the commutation relation $[a_{jk}, a_{jk}^{+}] = 1$

The Hamiltonian in Eq.3.26 can be written as

$$H_0 = \frac{\hbar\omega}{2}\sum_{k=x,y}^{N}\sum_{j=1}^{N}(\pi_{jk}^2 + q_{jk}^2) \tag{3.30}$$

$$= \sum_{k=x,y}^{N}\sum_{j=1}^{N}\left[\frac{1}{\sqrt{2}}(q_{jk}^{+} - i\pi_{jk}^{+})\frac{1}{sqrt2}(q_{jk} + i\pi_{jk}) + \frac{1}{2}\right]\hbar\omega \tag{3.31}$$

$$= \sum_{k=x,y}^{N}\sum_{j=1}^{N}\left(a_{jk}^{+}a_{jk} + \frac{1}{2}\right)\hbar\omega. \tag{3.32}$$

We construct two more operations in terms of the above operators as follows:

$$a_k^{+} = \frac{1}{\sqrt{N}}\sum_{j=1}^{N}a_{jk}^{+} = \frac{1}{\sqrt{N}}\sum_{j=1}^{N}\sqrt{\frac{m\omega}{2\hbar}}\left(r_{jk} - i\frac{P_{jk}}{m\omega}\right), \tag{3.33}$$

$$a_k = \frac{1}{\sqrt{N}}\sum_{j=1}^{N}a_{jk} = \frac{1}{\sqrt{N}}\sum_{j=1}^{N}\sqrt{\frac{m\omega}{2\hbar}}\left(r_{jk} + i\frac{P_{jk}}{m\omega}\right). \tag{3.34}$$

The Hamiltonian is finally given by

$$H_0 = \sum_{k=x,y}\left((a_k^{+}a_k + \frac{1}{2}\right)\hbar\omega \tag{3.35}$$

$$= \left(a_{jx}^{+}a_{jx} + \frac{1}{2}\right)\hbar\omega + \left(a_{jy}^{+}a_{jy} + \frac{1}{2}\right)\hbar\omega. \tag{3.36}$$

And the energy assumes the following expressions

$$E_0 = \left(n_x + \frac{1}{2}\right)\hbar\omega + \left(n_y + \frac{1}{2}\right)\hbar\omega. \tag{3.37}$$

So far we have ignored the Coulomb repulsion between the electrons. Let us switch on the electron

- electron interaction so that the total Hamiltonian becomes

$$H = H_0 + U, \tag{3.38}$$

where

$$U = \sum_{i<j=1}^{N} U\left(|\vec{r}_i - \vec{r}_j|\right) = \sum_{i<j=1}^{N} \frac{e^2}{\epsilon|\vec{r}_i - \vec{r}_j|}. \tag{3.39}$$

It is easy to prove that

$$\left[U\left(|\vec{r}_i - \vec{r}_j|\right), a_k^+\right] = \left[U\left(|\vec{r}_i - \vec{r}_j|\right), a_k\right] = 0. \tag{3.40}$$

This is true for any potential which depends only on the relative distance between electrons.Now

$$[H, a_k^+] = [H_0 + U(|\vec{r_i} - \vec{r_j}|), a_k^+] = [H_0, a_k^+] \tag{3.41}$$

$$= \hbar\omega \left[\sum_k \left(a_k^+ a_k + \frac{1}{2}\right), a_k^+\right] = \hbar\omega[(a_k^+ a_k, a_k^+)]. \tag{3.42}$$

Since

$$[a_k, a_k^+] = 1, \tag{3.43}$$

we have

$$[H, a_k^+] = \hbar\omega a_k^+, \tag{3.44}$$

$$[H, a_k] = -\hbar\omega a_k. \tag{3.45}$$

Suppose $\Phi(r)$ is an eigen function of H with eigenvalue E. Then

$$H\Phi(r) = E\Phi(r). \tag{3.46}$$

Now according to Eq.3.44 we can write

$$[H, a_k^+]\Phi(r) = \hbar\omega^+\Phi(r), \tag{3.47}$$

so that,

$$Ha_k^+\Phi(r) - a_k^+H\Phi(r) = \hbar\omega a_k^+\Phi(r), \tag{3.48}$$

or,

$$Ha_k^+\Phi(r) = (E + \hbar\omega)a_k^+\Phi(r). \tag{3.49}$$

Similarly we can show that

$$Ha_k\Phi(r) = (E - \hbar\omega)a_k\Phi(r). \tag{3.50}$$

Thus if $\Phi(r)$ is an eigen function of H with an eigen value E and then $a_k\Phi(r)$ is also an eigen function of H with eigenvalue $(E + \hbar\omega)$. Therefore the excitation spectrum of the interacting system consists of equidistant levels with separation equal to the bare resonance energy of the parabolic potential $(\hbar\omega)$. Thus electron-electron interaction does not alter the separation between the energy levels and hence the cyclotron frequency if the confinement potential is parabolic.

Peeters[17] has shown that the positions of the resonance lines in the magneto - optical absorption of a quantum dot with a system of electrons with a parabolic confinement potential is independent of the electron - electron interaction and the number of electrons in a quantum dot. We shall now discuss about this result which is known as **generalized Kohn's Theorem**.

In the presence of a magnetic field is in the z - direction, $\vec{p}_j$ is to be replaced by $\left(\vec{p}_j - \frac{e\vec{A}}{c}\right)$. In

the symmetric gauge we choose

$$\vec{A}_j = (y_j, x_j, 0)\frac{B}{2}. \tag{3.51}$$

It is easy to see that the Hamiltonian H_0 can still be diagonalized and one gets

$$H_0 = \left(d_1^+ d_1 + \frac{1}{2}\right)\hbar\omega_1 + \left(d_2^+ d_2 + \frac{1}{2}\right)\hbar\omega_2, \tag{3.52}$$

where

$$\omega_{1,2}^2 = \frac{1}{2}\left[(2\omega^2 + \omega_c^2) \pm \sqrt{(2\omega^2 + w_c^2)^2 - 4\omega^4}\right],$$

and,

$$d_{1,2}^{\pm} = \sum_{j=1}^{N} c_{1,2}^{\pm}(j),$$

with

$$c_{1,2}^{\pm} = u_{1,2}\left\{x_j\left(-\omega_{1,2}^2 + \omega^2 + \frac{1}{2}\omega_c^2\right) \mp i\frac{p_{jx}}{m\omega_{1,2}}(-\omega_{1,2}^2 + \omega^2) \mp iy_j\frac{\omega_c}{2\omega_{1,2}}(\omega_{1,2}^2 + \omega^2) - \frac{p_{jy}}{m}\omega_c\right\}, \tag{3.53}$$

where

$$u_{1,2} = \sqrt{\frac{m\omega_{1,2}}{2\hbar}}\left[(\omega_{1,2}^2 - \omega^2)^2 + \omega_c^2\omega^2\right].$$

One can easily verify that

$$[c_1^{\pm}(j), c_2^{\pm}(j)] = 0, \tag{3.54}$$

$$[c_S^{\pm}(j), c_S^{\pm}(j)] = 1 \qquad for \quad S = 1, 2. \tag{3.55}$$

Thus one would conclude that the excitation spectrum of system of electrons in a magnetic field and confined by a parabolic potential consists of two sets of equidistant levels with separations equal to w_1 and w_2.

Now again one can show that

$$[U, d^{\pm}_{1,2}] = 0, \tag{3.56}$$

so that we can get

$$[H, d^{\pm}_{1,2}] = \pm\hbar\omega_{1,2} d^{\pm}_{1,2}. \tag{3.57}$$

Thus also for an interacting electron gas in a magnetic field and confined by a parabolic potential the separation of the energy levels is identical to that in the absence of the electron - electron interaction. This is known as generalized Kohn's Theorem. This theorem along with the results of cyclotron resonance experiments suggest that the confinement potential in a quantum dot is parabolic.

After one comes to know about the form of the confining potential, applying quantum mechanics to a quantum dot problem becomes rather straight-forward and consequently a large number of theoretical investigations [18, 19, 20, 21, 22, 23, 24, 25, 26, 27, 28, 29, 30, 31, 32, 33, 34, 35, 36, 37, 38, 39, 40] were performed in the last twenty years to unravel the electronic and optical properties of quantum dots.

Chapter 4

Two electron system in a parabolic quantum dot in a magnetic field

The electronic properties of two-dimensional quantum dots are of considerable current interest. The theoretical studies are based on the model electron confinement, usually described by a parabolic potential. All the results provided by this model are in good agreement with experimental methods [41, 42, 43, 44], the main problem is that of how to take into account the electronelectron interaction. Here, we obtain the solution of the Schrodinger equation of a two-electron parabolic dot in an external magnetic field, making use of the WKB approximation.

4.1 The Model

The Hamiltonian for an interacting pair of electrons confined in a quantumdot by a parabolic potential of the form $(\frac{1}{2}m^*\omega_o^2\vec{r^2})$ in a magnetic field applied parallel to the z-axis(and perpendicular to the plane where the electrons are restricted to move)in the symmetric gauge is written as

$$H = \frac{1}{2m^*}[p_1 + \frac{e}{c}A(\vec{r_1})]^2 + \frac{1}{2}m^*\omega_0^2\vec{r_1}^2 + \frac{1}{2m^*}[p_2 + \frac{e}{c}A(\vec{r_2})]^2 + \frac{1}{2}m^*\omega_o^2\vec{r_2}^2 + \frac{e^2}{\epsilon}\frac{1}{|\vec{r_1} - \vec{r_2}|} \quad (4.1)$$

where the two-dimensional vectors $\vec{r_1}$ and $\vec{r_2}$ describes the positions the first and the second electron in the (x,y) plane respectively,and $\omega_c \left(= \frac{Be}{m^* c}\right)$ is the cyclotron frequency, ω_o is the characteristic confinement frequency, m^* is the effective mass of electron and ϵ is the dielectric constant of the medium.

4.2 The transformation into a One-Body problem

The following transformations are used for this problem:

$$\begin{aligned} \vec{P} &= \frac{1}{2}(\vec{p_1} + \vec{p_2}) & \vec{R} &= \frac{1}{2}(\vec{r_1} + \vec{r_2}) \\ \vec{p} &= \frac{1}{2}(\vec{p_1} - \vec{p_2}) & \vec{r} &= (\vec{r_1} - \vec{r_2}) \end{aligned} \tag{4.2}$$

where $\vec{R}$, $\vec{P}$ are the center-of-mass coordinates and $\vec{p}$, $\vec{r}$are the relative coordinates and taken $\hbar$=1.

Then

$$\vec{p} = -i\vec{\nabla}_r, \ \vec{P} = -i\vec{\nabla}_R$$

.

We also have

$$\begin{aligned} \vec{\nabla}_{r1} \times \vec{A}(\vec{r_1}) &= \vec{B}, \\ \vec{\nabla}_{r2} \times \vec{A}(\vec{r_2}) &= \vec{B}, \\ \text{and } \vec{A} &= \tfrac{1}{2}\vec{B} \times \vec{r} \end{aligned}$$

using the transformations (4.2) we get,

$$\frac{1}{2m^*}\left[p_1 + \frac{e}{c}A(\vec{r_1})\right]^2 + \frac{1}{2m^*}\left[p_2 + \frac{e}{c}A(\vec{r_2})\right]^2 = \frac{1}{2M}\left[P + \frac{Q}{c}A(\vec{R})\right]^2 + \frac{1}{2\mu}\left[p + \frac{q}{c}A(\vec{r})\right]^2 \tag{4.3}$$

and

$$\frac{1}{2}m^*\omega_o^2 r_1^2 + \frac{1}{2}m^*\omega_o^2 r_2^2 + \frac{e^2}{\epsilon}\frac{1}{|\vec{r}|} = \frac{1}{2}M\omega_o^2 R^2 + \frac{1}{2}M{\omega_o}^2 r^2 + \frac{e^2}{\epsilon}\frac{1}{|\vec{r}|} \tag{4.4}$$

The Hamiltonian in equation (4.1) can be written as sum of two seperable hamiltonians, one representing the centre-of-mass motion and given by

$$H_R = \frac{1}{2M}\left[P + \frac{Q}{c}A(\vec{R})\right]^2 + \frac{1}{2}M\omega_o^2 R^2 \tag{4.5}$$

and the other representing the relative motion and is given by

$$H_r = \frac{1}{2\mu}\left[p + \frac{q}{c}A(\vec{r})\right]^2 + \frac{1}{2}\mu{\omega_0}^2 r^2 + \frac{e^2}{\epsilon}\frac{1}{|\vec{r}|} \tag{4.6}$$

where $M = 2m^*$, $Q = 2e$, $\mu = \frac{1}{2}m^*$ and $q = \frac{1}{2}e$.

Thus the total Hamiltonian is given by

$$H = H_R + H_r \tag{4.7}$$

In experimentally realized dots, the motion in the z-direction is always frozen, and we can treat the dots as two-dimensional discs using a parabolic confinement potential, as usual.

The total wavefunction for the above hamiltonian can be written as

$$\Psi = \Phi(\vec{R})\phi(\vec{r}) \tag{4.8}$$

where $\Phi(\vec{R})$ and $\phi(\vec{r})$ satisfy the following equations:

$$H_R\Phi(\vec{R}) = E_c\Phi(\vec{R}) \tag{4.9}$$

$$H_r\phi(\vec{r}) = E_r\phi(\vec{r}) \tag{4.10}$$

We choose the gauge as $A_\varphi = \frac{1}{2}Br,\ A_r = A_z = 0$.

Then in the polar coordinates, the Hamiltonian H_r takes the form

$$H_r = -\frac{1}{2\mu}\left[\frac{1}{r}\frac{\partial}{\partial r}(r\frac{\partial}{\partial r}) + \frac{1}{r^2}\frac{\partial^2}{\partial\varphi^2}\right] + \frac{1}{2}\mu\Omega^2r^2 - \frac{i}{2}\omega_c\frac{\partial}{\partial\varphi} + \frac{e^2}{\varepsilon r}, \tag{4.11}$$

with the cyclotron frequency given by $\omega_c = \frac{Be}{m^*c}$ and the renormalized confinement frequency Ω given by $\Omega^2 = \omega_o^2 + \frac{{\omega_c}^2}{4}$. The dielectric constant ε concerns the host semiconductor. After making the substitution $\phi(r) = r^{-\frac{1}{2}}\chi(r)\exp(im\varphi)$, we obtain

$$\frac{d^2\chi(r)}{dr^2} + \left(2\mu E_r - m\mu\omega_c - \frac{m^2 - \frac{1}{4}}{r^2} - \mu^2\Omega^2r^2 - \frac{2\mu e^2}{\varepsilon}\frac{1}{r}\right)\chi(r) = 0 \tag{4.12}$$

where m=0, $\pm$1, $\pm$2,.... denotes the azimuthal quantum number

The centre-of-mass wave function $\Phi(R)$ can be exactly solved in terms of the confluent hypergeometric function. The spectrum is

$$E_c = (2N + |\mathrm{M}| + 1)\Omega + \frac{1}{2}\mathrm{M}\omega_c, \tag{4.13}$$

where N=0, 1, 2, 3, ... and M=0, $\pm$1, $\pm$2, ...

In the following we concentrate on the relative motion only. After making the substitution $r = \sqrt{2}lx$, where $l^2 = \frac{1}{m^*\Omega}$, we get from Eq:(4.12)

$$\frac{d^2\chi(x)}{dx^2} + \left(\epsilon - x^2 - \frac{\beta}{x} - \frac{\gamma}{x^2}\right)\chi(x) = 0 \tag{4.14}$$

with $\epsilon = \frac{2E_r - m\omega_c}{\Omega}$, $\gamma^2 = m^2 - \frac{1}{4}$, $\beta = \frac{\sqrt{2}l}{\epsilon a_B}$ and $a_B = \frac{1}{m^* e^2}$

4.3 WKB Method for 2D PQD

We solve (4.14) using the WKB approximation following[1]. The WKB approximation is the most familiar example of a semiclassical calculation in quantum mechanics in which the wavefunction is recast as an exponential function, semiclassically expanded, and then either the amplitude or the phase is taken to be slowly changing.The important contribution of Wentzel, Kramers and Brillouin to the Jeffreys method was the inclusion of the treatment of turning points, connecting the evanescent and oscillatory solutions at either side of the turning point. For example, this may occur in the Schrdinger equation, due to a potential energy hill.

Equation (4.14) contains the irregular singularity at x=0. According to the general WKB theory for equations with irregularities one needs replace γ by $\gamma + \frac{1}{4}$. Thereafter, the semiclassical spectrum of the system can be obtained from the Bohr–Sommerfeld condition

$$\int_a^b \left(\epsilon - x^2 - \frac{\beta}{x} - \frac{m^2}{x^2}\right) dx = \pi(n + \frac{1}{2}), \tag{4.15}$$

where the turning points a, b are determined by the positive roots of the algebraic equation

$$x^4 - \epsilon x^2 + \beta x + m^2 = 0. \tag{4.16}$$

The solution of equation (4.16) can be easily carried out numerically by using MATLAB. From

this equation ϵ value can be calculated and substituted in the energy equation given by

$$E_r = \frac{\epsilon\Omega + m\omega_c}{2} \tag{4.17}$$

The total energy thus becomes

$$E = (2N + |\mathrm{M}| + 1)\Omega + \frac{1}{2}\mathrm{M}\omega_c + \frac{\epsilon\Omega + m\omega_c}{2} \tag{4.18}$$

4.4 Results and Discussions

For noninteracting electrons, $\beta = 0$, the numerical WKB solution coincides precisely with the exact numerical solutions repeated in [1].We present these results in Figure:(4.1). The energy as a function of the magnetic field shows a minimum at some value of the magnetic field.This minimum becomes deeper and deeper with increasing m and also shifts to the high magnetic field.

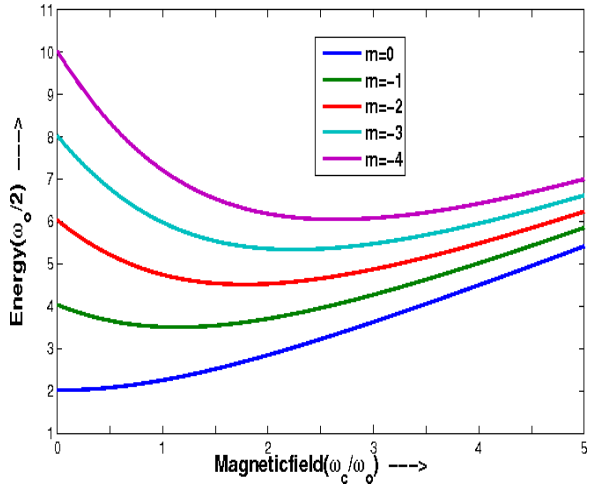

Figure 4.1: The spectrum of a two-electron quantumdot(parabolic potential) in the WKB approximation for n=0 and m=0,-1,-2,-3,-4 and in the absence of electron-electron interaction .$\beta = 0$

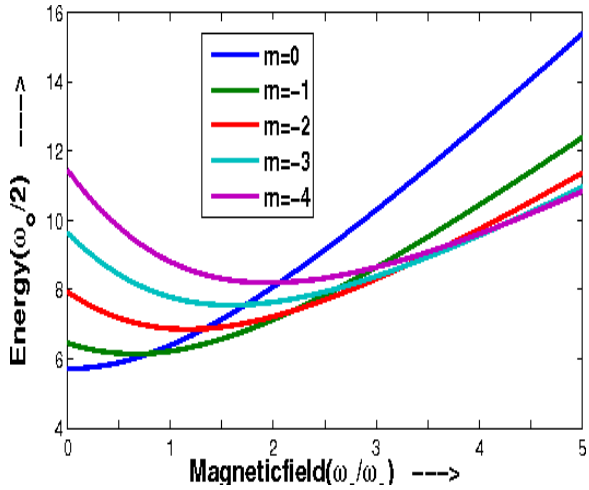

Figure 4.2: The spectrum of a two-electron quantumdot(parabolic potential) in the WKB approximation for n=0 and m=0,-1,-2,-3,-4 and in the presence of electron-electron interaction.$\beta = 3$. The ground state shifts to the states with higher angular momentum as the magnetic field increases.

As the magnetic field strength increases the energy of the states $m = 0$ increases while the energy of the states with non-vanishing quantum number m decreases. This leads to a sequence of different ground states with $m = 0,\ -1,\ -2\ \ldots$ with an increase in magnetic field. Similar behaviour is observed for higher excited states also, but at higher magnetic fields. These give raise to an interesting phenomenon of energy level corssing. This happens because the coulomb energy gets smaller and smaller when the angular momentum $|m|$ along with the average distance between the electrons.

In Figure:4.3 we compare the energy of two electron system in a magnetic field for $\beta = 0$ and $\beta = 3$. One can easily observe that for $\beta = 3$ the energy is higher. This is understandable because the electron-electron interaction is supposed to increase the total energy.

In Figure:4.4 we plot the ground state energy of the system as a functionm of dot size. for $\beta = 0$ and for $\beta = 3$. It is clearly evident that other parameters remaining same, the electron-electron interaction increases the energy of the two-electron system.

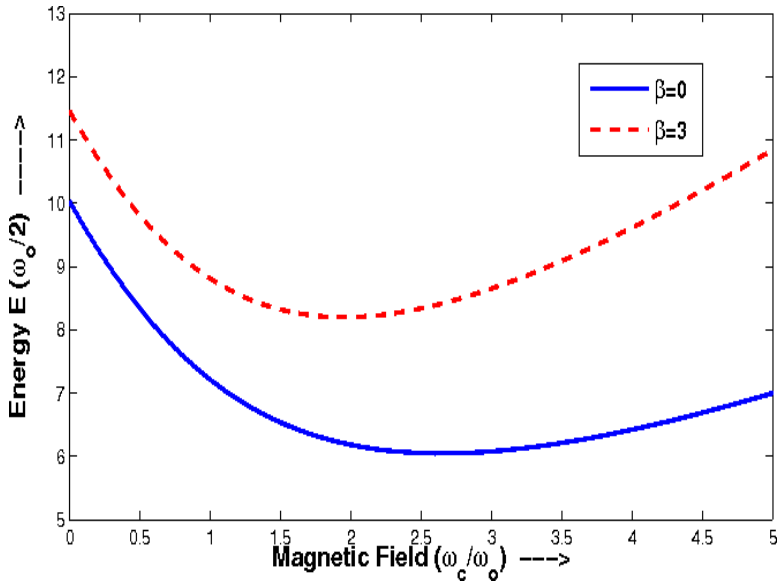

Figure 4.3: Comparison of total energy of two electron system in a quantum dot with parabolic confinement including electron-electron interaction (dashed curve) and without including electron-electron interaction (solid curve) as a function of magnetic field for $V_o = 100$

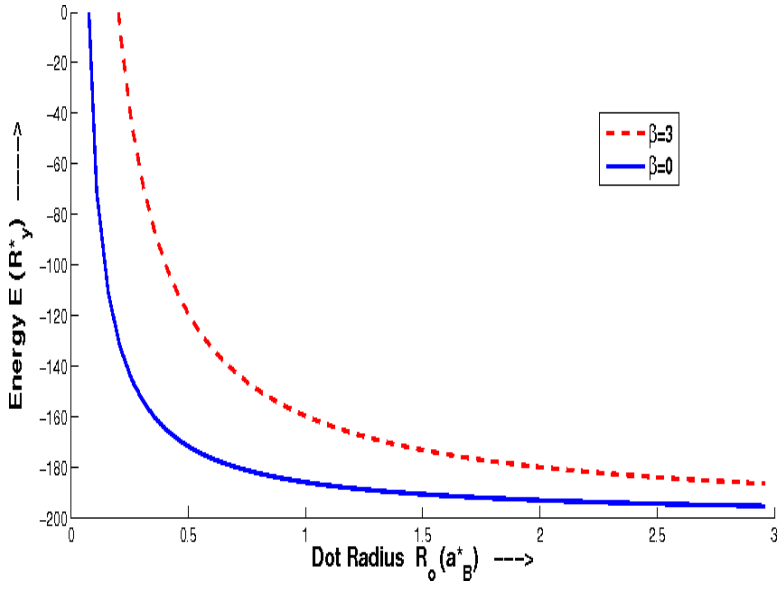

Figure 4.4: Comparison of total energy of two electron system in a quantum dot with parabolic confinement including electron-electron interaction (dashed curve) and without including electron-electron interaction (solid curve) as a function of dot size for $V_o = 100$

In order to compare the effect of confinement geometry on the total energy, we present in Fig:4.5 the behaviour of the ground state energy of the two electron system $2D$ disc-like and $3D$ spherical quantum dots .

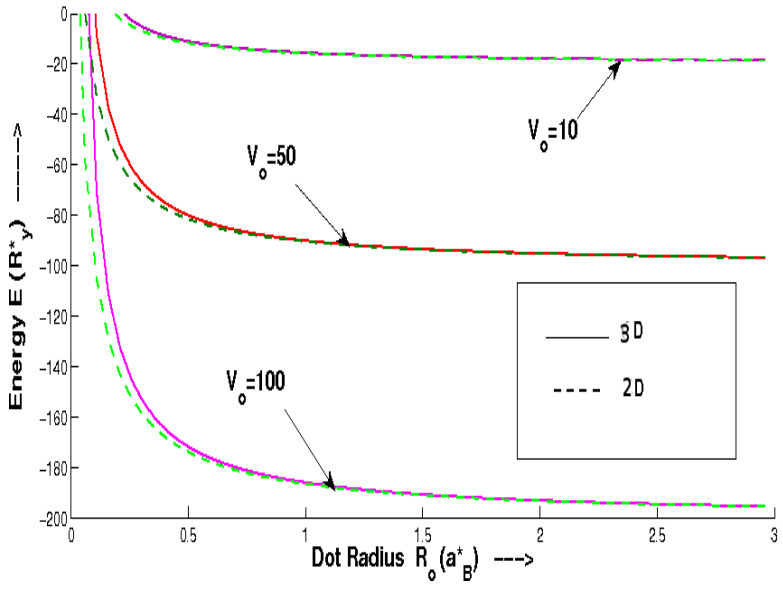

Figure 4.5: Comparison of total energy of two electron system in a quantum dot with parabolic confinement in two dimensions(dashed curves) and three dimension (solid cueves) as a function of quantum dot size for three values of V_o.

The energy increases very rapidly with decreasing quantum dot raduis below a certain value of the dot size for $2D$ and $3D$ systems, of course, with a quantitative difference. In other words, for smaller values of the dot radius, the energy of a QD is more sensitive to the size of the dot. In the case of small dot size, spatial overlap between the two electrons incerases, which leads to the enhancement of Coulumb binding energy. As the dot size becomes very large, the confinement becomes weak and energy of the system approaches to that of bulk counterpart. Again one can easily see that the total energy is lower in a $2D$ dot as compared to the $3D$ structure. The reason for this situation is the contribution coming from the extra degree of freedom in the third direction. Further more as the depth of the potential increases, energy becomes lower and lower.

Chapter 5

Two electron system in a gaussian quantum dot in a magnetic field

5.1 Introduction

In Chapter 3 we have shown that the confinement potential in a quantum dot is more or less parabolic. We have therefore considered in Chapter 4 a quantum dot with parabolic confinement and studied the energy of a system of two electrons in such a quantum dot in the presence of a magnetic field. The parabolic confinement potential has also been used by several other authors during the last two decades to study some of the electronic and optical properties of quantum dots. However some recent experiments have revealed that the confinement potential in a quantum dot is not really parabolic but is rather anharmonic. Adamowsky has recently suggested that a Gaussian potential can work as a confinement potential for a quantum dot with a good amount of accuracy. Quite a few investigations have followed after this suggestion. In the present chapter we shall take up the same problem of a system of two electrons and study the energy of a such a system in a Gaussian quantum dot (GQD).

5.2 The Model

The Hamiltonian of a system of two electrons confined in a quantum dot with Gaussian potential and placed in a magneticfield is given by

$$\begin{aligned} H &= \frac{1}{2m^*}\left[p_1 + \frac{e}{c}A(r_1)\right]^2 + \frac{1}{2}m^*\omega_0^2 r_1^2 + \frac{1}{2m^*}\left[p_2 + \frac{e}{c}A(r_2)\right]^2 + \frac{1}{2}m^*\omega_0^2 r_2^2 \\ &\quad -V_o e^{-\frac{r_1^2}{2R_o^2}} - V_o e^{-\frac{r_2^2}{2R_o^2}} + \frac{e^2}{\epsilon}\frac{1}{|\vec{r_1} - \vec{r_2}|}, \end{aligned} \tag{5.1}$$

where $V_o(V_o > 0)$ denotes the depth of the potential well, m^* is the effective mass of each electron, R is the range of the confinement potential which may be identified as the size of the QD, $\vec{r}_1$ and $\vec{r}_2$ are the position vectors of the first and the second electrons respectively, ϵ is dielectric constant of the medium, and $|\vec{r_1} - \vec{r_2}|$ separation between the two electrons.

For $r/R << 1$, The gaussian potential can be approximated by the parabolic potential as

$$V(r_i) = -V_o + \gamma^2 r_i^2, \tag{5.2}$$

where $\gamma^2 = V_o/2R^2$. This can be called as harmonic approximation.

5.3 Harmonic Approximation

We shall make a harmonic approximation which is different from (5.2). Adding $\frac{1}{2}m\omega_o^2 r_1^2$,$\frac{1}{2}m\omega_o^2 r_2^2$ and $2V_o$, to Equation:5.1 and subtacting the same terms, we obtain

$$\begin{aligned} H = \frac{1}{2m^*}\left[p_1 + \frac{e}{c}A(r_1)\right]^2 + \frac{1}{2}m\omega_o^2 r_1^2 + \frac{1}{2m^*}\left[p_2 + \frac{e}{c}A(r_2)\right]^2 + \frac{1}{2}m\omega_o^2 r_2^2 \\ + V_o - V_o e^{-\frac{r_1^2}{2R^2}} - \frac{1}{2}m\omega_o^2 r_1^2 + V_o \end{aligned} \tag{5.3}$$

$$- V_o e^{-\frac{r_2^2}{2R^2}} - \frac{1}{2} m\omega_o^2 r_2^2 + \frac{e^2}{\epsilon} \frac{1}{|\vec{r_1} - \vec{r_2}|} - 2V_o,$$

which can be written as

$$\begin{aligned} H = \frac{1}{2m^*} \left[p_1 + \frac{e}{c} A(r_1) \right]^2 + \frac{1}{2} m\omega_o^2 r_1^2 - \frac{1}{2m^*} \left[p_2 + \frac{e}{c} A(r_2) \right]^2 + \frac{1}{2} m\omega_o^2 r_2^2 \\ + \lambda \left(\frac{V_o}{r_1^2} - V_o \frac{e^{-\frac{r_1^2}{2R^2}}}{r_1^2} - \frac{1}{2} m\omega_o^2 \right) r_1^2 \\ + \lambda \left(\frac{V_o}{r_2^2} - V_o \frac{e^{-\frac{r_2^2}{2R^2}}}{r_2^2} - \frac{1}{2} m\omega_o^2 \right) r_2^2 \\ + \frac{e^2}{\epsilon} \frac{1}{|\vec{r_1} - \vec{r_2}|} - 2V_o. \end{aligned} \tag{5.4}$$

Where $\lambda = 0$ gives the two-electron problem in PQD, while $\lambda = 1$ corresponds to the problem in GQD. Now we shall make an approximation and write the Hamiltonian (5.4) as

$$\begin{aligned} H = \frac{1}{2m^*} \left[p_1 + \frac{e}{c} A(r_1) \right]^2 + \frac{1}{2} m\omega_o^2 r_1^2 + \frac{1}{2m^*} \left[p_2 + \frac{e}{c} A(r_2) \right]^2 + \frac{1}{2} m\omega_o^2 r_2^2 \\ + \lambda \left(\frac{V_o}{< r_1^2 >} - V_o \frac{\langle e^{-\frac{r_1^2}{2R^2}} \rangle}{< r_1^2 >} - \frac{1}{2} m\omega_o^2 \right) r_1^2 \\ + \lambda \left(\frac{V_o}{< r_2^2 >} - V_o \frac{\langle e^{-\frac{r_2^2}{2R^2}} \rangle}{< r_2^2 >} - \frac{1}{2} m\omega_o^2 \right) r_2^2 \\ + \frac{e^2}{\epsilon} \frac{1}{|\vec{r_1} - \vec{r_2}|} - 2V_o. \end{aligned} \tag{5.5}$$

where the averaging has to be suitably done. We can write the above Hamiltonian as

$$H = H_1 + H_2 + h_1 + h_2 + \frac{e^2}{\epsilon}\frac{1}{|\vec{r_1} - \vec{r_2}|} - 2V_o, \tag{5.6}$$

where

$$H_1 = \frac{1}{2m^*}\left[p_1 + \frac{e}{c}A(r_1)\right]^2 + \frac{1}{2}m\omega_o^2 r_1^2, \tag{5.7}$$

$$H_2 = \frac{1}{2m^*}\left[p_2 + \frac{e}{c}A(r_2)\right]^2 + \frac{1}{2}m\omega_o^2 r_2^2, \tag{5.8}$$

$$h_1 = \lambda\left(\frac{V_o}{< r_1^2 >} - V_o\frac{\langle e^{-\frac{r_1^2}{2R_o^2}}\rangle}{< r_1^2 >} - \frac{1}{2}m\omega_o^2\right) r_1^2, \tag{5.9}$$

$$h_2 = \lambda\left(\frac{V_o}{< r_2^2 >} - V_o\frac{\langle e^{-\frac{r_2^2}{2R_o^2}}\rangle}{< r_2^2 >} - \frac{1}{2}m\omega_o^2\right) r_2^2, \tag{5.10}$$

Now the averaging state in $< r_1^2 >$ and $\langle e^{-\frac{r_1^2}{2R_o^2}}\rangle$ is choosen to be the ground state wave function of H_1 and that in $< r_2^2 >$ and $\langle e^{-\frac{r_2^2}{2R_o^2}}\rangle$ to be the ground state wavefunction of H_2.

Since $< r_1^2 >=< r_2^2 >$, we have

$$\left(\frac{V_o}{< r_1^2 >} - V_o\frac{e^{-\frac{r_1^2}{2R_o^2}}}{< r_1^2 >} - \frac{1}{2}m\omega_o^2\right) = \left(\frac{V_o}{< r_2^2 >} - V_o\frac{e^{-\frac{r_2^2}{2R^2}}}{< r_2^2 >} - \frac{1}{2}m\omega_o^2\right) \equiv \omega_1^2,$$

so that the Hamiltonian (5.4) becomes

$$H = \frac{1}{2m^*}\left[p_1 + \frac{e}{c}A(r_1)\right]^2 + \frac{1}{2}m\left(\omega_o^2 + 2\frac{\lambda}{m}\omega_1^2\right) r_1^2$$

$$+\frac{1}{2m^*}\left[p_2+\frac{e}{c}A(r_2)\right]^2+\frac{1}{2}m\left(\omega_o^2+2\frac{\lambda}{m}\omega_1^2\right)r_2^2 \tag{5.11}$$

$$+\frac{e^2}{\epsilon}\frac{1}{|\vec{r_1}-\vec{r_2}|}-2V_o.$$

or,

$$H=\frac{1}{2m^*}\left[p_1+\frac{e}{c}A(r_1)\right]^2+\frac{1}{2m^*}\left[p_2+\frac{e}{c}A(r_2)\right]^2+\frac{1}{2}m^*\omega^2r_1^2+\frac{1}{2}m^*\omega^2r_2^2+\frac{e^2}{\epsilon}\frac{1}{|\vec{r_1}-\vec{r_2}|}-2V_o. \tag{5.12}$$

where $\omega^2=\omega_o^2+2\frac{\lambda}{m}\omega_1^2$. The above Hamiltonian is similar to the earlier Hamiltonian (Equation:4.1) except $-2V_o$ term which is just a constant.

5.3.1 The transformation into a One-Body problem

As in 4.2 we perform the following transformations :

$$\vec{P}=\frac{1}{2}(\vec{p_1}+\vec{p_2}),\qquad \vec{R}=\frac{1}{2}(\vec{r_1}+\vec{r_2})$$
$$\vec{p}=\frac{1}{2}(\vec{p_1}-\vec{p_2}),\qquad \vec{r}=(\vec{r_1}-\vec{r_2}) \tag{5.13}$$

We then have$\vec{p}=-i\vec{\nabla}_r$, $\vec{P}=-i\vec{\nabla}_R$, where we have taken $\hbar$=1.

where $\vec{R},\vec{P}$ are the center-of-mass variables and $\vec{p},\vec{r}$are the relative variables.

Using the transformations (5.13) the Hamiltonian can be separated into the center-of-mass and relative-motion parts as follows:

$$H=H_R+H_r \tag{5.14}$$

Where

$$H_R = \frac{1}{2M}\left(P + \frac{Q}{c}A(R)\right)^2 + \frac{1}{2}M\gamma^2 R^2 \tag{5.15}$$

$$H_r = \frac{1}{2\mu}\left(P + \frac{q}{c}A(r)\right)^2 + \frac{1}{2}\mu\gamma^2 r^2 + \frac{e^2}{\epsilon}\frac{1}{|r|} - 2V_0 \tag{5.16}$$

with $M = 2m^*$, $Q = 2e$, $\mu = \frac{1}{2}m^*$,$q = \frac{1}{2}e$ and γ is the renormalized confinement frequency given by

$$\gamma^2 = \omega^2 + \frac{\omega_c^2}{4} \tag{5.17}$$

where ω_c is the cyclotron frequency given by $\omega_c = \frac{eB}{m^*c}$

We choose the gauge for the vector potential as $A_\varphi = \frac{1}{2}Br$, $A_r = A_z = 0$. In the polar coordinates, the Hamiltonian of the relative motion takes the form

$$H_r = -\frac{1}{2\mu}\left[\frac{1}{r}\frac{\partial}{\partial r}(r\frac{\partial}{\partial r}) + \frac{1}{r^2}\frac{\partial^2}{\partial\varphi^2}\right] + \frac{1}{2}\mu\gamma^2 r^2 - \frac{i}{2}\omega_c\frac{\partial}{\partial\varphi} + \frac{e^2}{\epsilon r} - 2V_0. \tag{5.18}$$

The total wave function for the problem described by H (eq.(5.14))can be written as

$$\Psi = \Phi_c(\vec{R})\phi_r(\vec{r}) \tag{5.19}$$

where $\Phi_c(\vec{R})$ and $\phi_r(\vec{r})$ satisfy the equations

$$H_c\Phi_c(\vec{R}) = E_c\Phi_c(\vec{R}) \tag{5.20}$$

$$H_r\phi_r(\vec{r}) = E_r\phi_r(\vec{r}) \tag{5.21}$$

Eq.(5.20)can be solved exactly and the energy spectrum is given by

$$E_c = (2N + |\mathrm{M}| + 1)\gamma + \frac{1}{2}\mathrm{M}\omega_c \tag{5.22}$$

Where N=0, 1, 2, 3, ... M=0, ±1, ±2, ... we shall now concentrate on the relative motion.

After making the substitution $\phi_r(\vec{r}) = r^{-\frac{1}{2}}\chi(r)\exp(im\varphi)$ in Eq(), we obtain

$$\frac{d^2\chi(r)}{dr^2} + \left(2\mu E - m\mu\omega_c + 4\mu V_0 - \frac{m^2 - \frac{1}{4}}{r^2} - \mu^2\gamma^2 r^2 - \frac{2\mu e^2}{\epsilon}\frac{1}{r}\right)\chi(r) = 0 \tag{5.23}$$

where m denotes the azimuthal quantum number which can take values 0, ±1, ±2, ...

.After making the substitution $r = \sqrt{2}lx$, where $l^2 = \frac{1}{m^*\omega}$, we get from Eq.(5.23)

$$\frac{d^2\chi(x)}{dx^2} + \left(\epsilon - x^2 - \frac{\beta}{x} - \frac{\gamma}{x^2}\right)\chi(x) = 0 \tag{5.24}$$

with

$$\epsilon = \frac{2E_r - m\omega_c + 4V_0}{\gamma},\ \gamma = (m^2 - \frac{1}{4}),\ \beta = \frac{\sqrt{2}l}{\epsilon a_B},\ a_B = \frac{1}{m^* e^2}$$

5.3.2 WKB Solution:

As before we shall solve equation (5.24) within the framework of the WKB approximation. Equation (5.24) contains the irregular singularity at x=0. According to the general WKB theory for equations with irregular singularities one needs to replace γ by $\gamma + \frac{1}{4}$. Thereafter, the semiclassical spectrum of the system can be obtained from the Bohr-Sommerfeld condition

$$\int_a^b \left(\epsilon - x^2 - \frac{\beta}{x} - \frac{m^2}{x^2}\right)dx = \pi(n + \frac{1}{2}), \tag{5.25}$$

where the turning points a, b are determined by the positive roots of the algebraic equation

$$x^4 - \epsilon x^2 + \beta x + m^2 = 0. \tag{5.26}$$

The solution of Eq.(5.25) can be easily carried out numerically by using MATLAB and MATHEMATICA. From this ϵ value can be calculated and substituted in the energy equation given by:

$$E_r = \frac{\epsilon\gamma + m\omega_c - 4V_0}{2}. \tag{5.27}$$

The total energy E is given by sum of E_c and E_r. Thus we get

$$E = (2N + |\mathrm{M}| + 1)\gamma + \frac{1}{2}\mathrm{M}\omega_c + \frac{\epsilon\gamma + m\omega_c - 4V_0}{2} \tag{5.28}$$

5.4 Results and Discussions:

For noninteracting electrons $\beta = 0$, the corresponding numerical WKB solutions for the energies are presented in Figure:5.1 as a function of the ratio $\frac{\omega_c}{\omega_o}$.

As in the case of PQD, here also the minimum structure is clearly visible. As the magnetic field strength increases the energy of the states $m = 0$ increases while the energy of the states with non-vanishing quantum number m decreases. This leads to a sequence of different ground states with $m = 0,\ -1,\ -2\ \ldots$ with an increase in magnetic field. Similar behaviour is observed for higher excited states also, but at higher magnetic fields. These give raise to an interesting phenomenon of energy level corssing. This happens because the coulomb energy gets smaller and smaller when the angular momentum $|m|$ along with the average distance between the electrons.

In Figure:5.3 we compare the energy of two electron system in a magnetic field for $\beta = 0$ and $\beta = 3$. One can easily observe that for $\beta = 3$ the energy is higher. This is understandable because

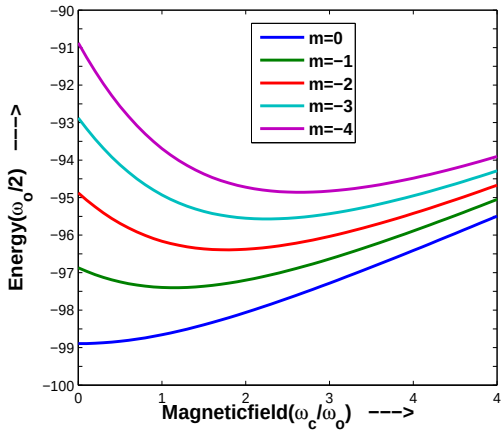

Figure 5.1: The spectrum of a two-electron quantumdot(gaussian potential) in the WKB approximation for n=0 and m=0,-1,-2,-3,-4 and in the absence of electron-electron interaction .$\beta = 0$

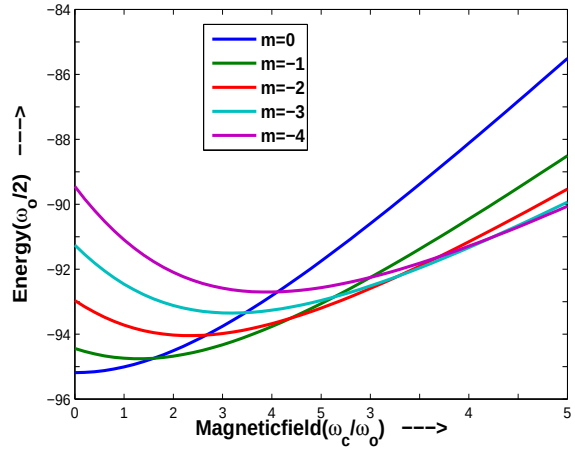

Figure 5.2: The spectrum of a two-electron quantumdot(gaussian potential) in the WKB approximation for n=0 and m=0,-1,-2,-3,-4 and in the absence of electron-electron interaction.$\beta = 3$. The ground state shifts to the states with higher angular momentum as the magnetic field increases.

the electron-electron interaction is supposed to increase the total energy. This result is similar to that obtained in the case of parabolic confinement potential.

In Figure:4.4 we plot the ground state energy of the system as a functionm of dot size. for $\beta = 0$

and for $\beta = 3$. It is clearly evident that other parameters remaining same, the electron-electron interaction increases the energy of the two-electron system.

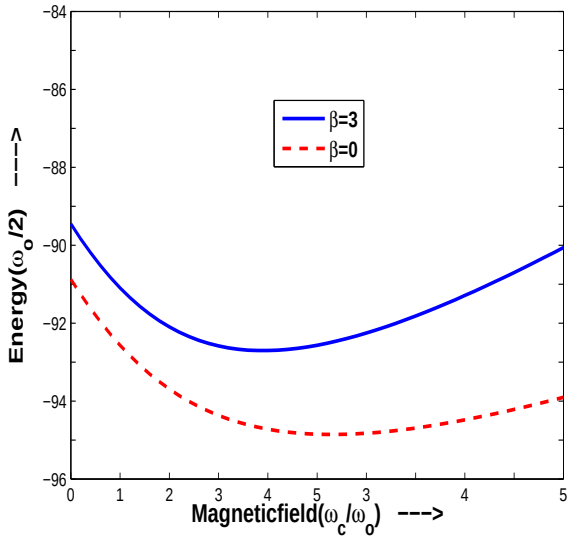

Figure 5.3: Comparison of total energy of two electron system in a quantum dot with parabolic confinement including electron-electron interaction (dashed curve) and without including electron-electron interaction (solid curve) as a function of magnetic field for $V_o = 100$

The spectra of the interacting electrons are shown in figure(4.2) for $\beta = 3$. As the magnetic field increases, the ground state $n = 0, m = 0$ shifts to the levels with higher angular momentum $n = 0, m = -1, -2, -3, ...$ This happens because the Coulomb energy gets smaller when the angular momentum $|m|$ increases along with the average distance between electrons. The same thing one can observe in Fig:4.3 also for $m = -4,\ \beta = 0, 3$

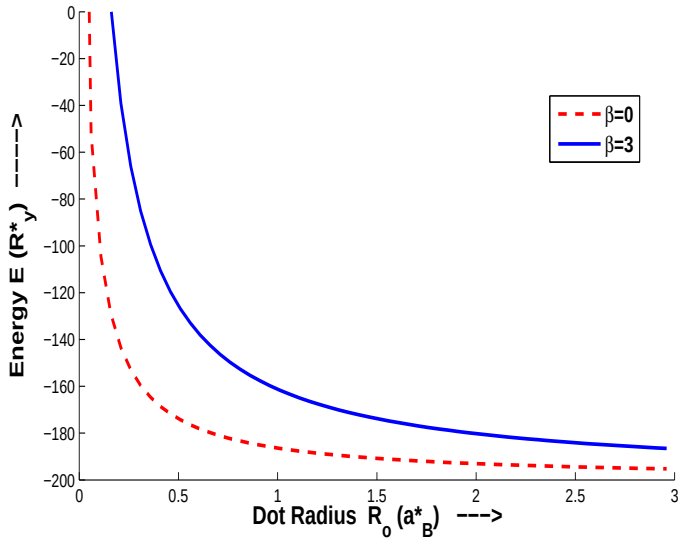

Figure 5.4: Comparison of total energy of two electron system in a quantum dot with parabolic confinement including electron-electron interaction (dashed curve) and without including electron-electron interaction (solid curve) as a function of quantum dot size for $V_o = 100$

In order to compare the effect of confinement geometry on the total energy, we present in Fig:4.5 the behaviour of ground state energy of two electron system in a parabolic quantum dot in presence of magnetic field for $2D$ disc-like and $3D$ spherical quantum dots as a function of the dot size. This is similar to the results with parabolic confinement qualitatively, but quantutatively a little higher.

The energy increases very rapidly with decreasing quantum dot raduis below a certain value of radius both for $2D$ and $3D$ systems, of course, with a quantitative difference. In otherwords, for smaller values of radius, the energy of the system is more sensitive to the size of the dot. in the case of small dot size, spatial overlap between the two electrons incerases, which leads to the enhancement of Coulumb binding energy. As the dot size becomes very large, the confinement becomes weak and energy of the system approaches to that of bulk counterpart. The total energy of two electron system in a $2D$ disc-like quantum dot is lowewr than that in the $3D$ spherical

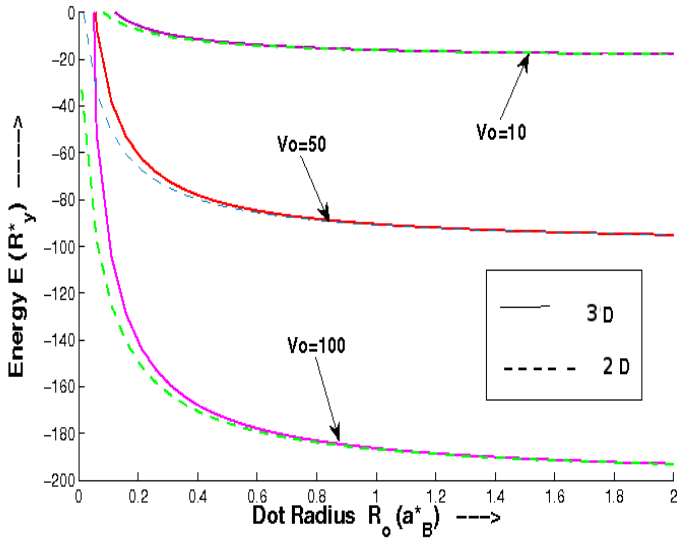

Figure 5.5: Comparison of total energy of two electron system in a quantum dot with parabolic confinement in two dimensions(dashed curves) and three dimension (solid cueves) as a function of quantum dot size for three values of V_o.

quantum dot for the same radius. The reason for this situation is the contribution coming from the extra degree of freedom in the third direction. Furthermore, as the depth of the potential increases, energy becomes lower and lower.

Figure(5.6) shows the total energy as a function of dot size for a two-dimensional gaussian(solid curves) and parabolic (dashed curve) quantum dot for different V_o. The qualitative properties of energy levels for the gaussian potential and the parabolic potential are similar. However, the quantitative differences are also obvious. In the strong confinement case the energies in the gaussian potential are obviously lower than those in the parabolic potential. Thus parabolic potential overestimates the energy compared to the Gaussian potential. The energy difference between the gaussian potential and the parabolic potential fast increases as the dot radius decreases. When quantum dot size is larger, the calculation values of both the gaussian potential and the parabolic potential are reaching consistent, i.e. only for a larger quantum dot can the parabolic be regarded as a fairly

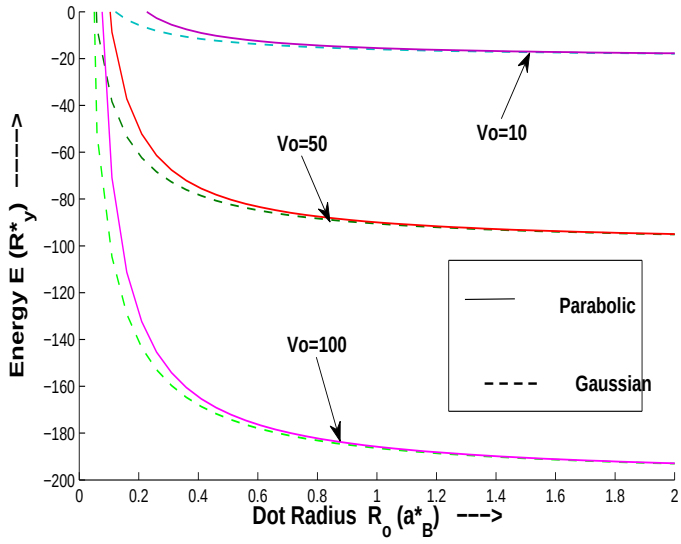

Figure 5.6: Comparison of total energy of two electron system in a 2D-quantum dot with Gaussian confinement (dashed curves) and Parabolic confinement (solid cueves) as a function of quantum dot size for three values of V_o.

good approximation of the nonparabolic gaussian potential.

Chapter 6

Conclusion

In this dissertation we have first given an overview of the subject of the quantum dots in a modest way. We have described several fabrication techniques that are commonly used in the laboratory. We have discussed the concept of the charge quantization in quantum dots and introduced the phenomena of Coulomb blocked which is expected to play an important role in single electron transistors.

One of the important issues that one has to worry about while dealing with a quantum dot is the nature of the confinement potential. In fact, cyclotron resonance experiments together with what is known as the generalized Kohn theorem have suggested that the confinement potential in a quantum dot is more or less parabolic in nature. We have therefore first considered the two-electron problem in a quantum dot in a magnetic field with parabolic confinement in 2D. The problem could be separated into a center of mass part and a relative coordinate part. The center of mass part is found to be exactly soluble, but the relative motion part does not admit an analytic solution. We have solved it by using WKB approximation to obtain the ground state energy.

Following S.Klama[1], these results are in excellent agreement with the exact numerical results. We have therefore extended the work to $3D$ and studied the effect of size of the dot and depth of

the confinement potential and the magnetic field on the total energy of the two electron system. Here we have shown that the total energy is, in general, higher in $3D$ than in $2D$ for fixed dot parameters. This is due to the extra contribution coming from the motion in the third dimension in a $3D$ dot. Furthermore, as the depth of the potential increases, energy becomes lower and lower.

Some recent experiments have revealed that the confinement potential in a quantum dot is not really parabolic but is actually anharmonic with a minimum structure and it has been suggested in this context that a Gaussian potential is a much better choice. We have therefore next taken up the same problem of the two-electron system in a magnetic field with Gaussian confinement. We have also compared our results with those of a corresponding parabolic quantum dot. The results obtained for a Gaussian quantum dot are qualitatively similar to those obtained for parabolic quantum dot. However, Our calculations show that though for large quantum dots, the parabolic potential model works fairly well, for a small dot it is only a poor approximation of the more realistic Gaussian confinement potential model. In general, the parabolic model overestimates the energy. We have performed calculations for both two and three dimensional quantum dots and have shown that the ground state energy is lower in a two-dimensional Gaussian dot as in a parabolic dot.

Bibliography

[1] S. Klama and E.G. Mishchenko, J. Phys.: Condens. Matter 10, 3411 (1998)

[2] Reed M A, Bate R T, Bradshaw K, Duncan W M, Frensley W M, Lee J W and Smith H D 1986 J. Vac. Sci.Technol. B 4 358

[3] Ashoori R C 1996 Nature 379 413

[4] Hansen W, Smith T P, Lee K Y, Brum J A, Knoedler C M, Hong J M and Kern D P 1989 Phys. Rev. Lett. 62 2168

[5] Lorke A, Kotthaus J P and Ploog K 1990 Phys. Rev. Lett. 64 2559

[6] Zhitenev N B, Brodsky M, Ashoori R C, Pfeiffer L N and West K W 1999 Science 285 715

[7] Fukui T, Ando S and Tokura Y 1991 Appl. Phys. Lett. 58 2018

[8] C. A. Leatherdale, W.-K. Woo, F. V. Mikulec, and M. G. Bawendi - On the Absorption Cross Section of CdSe Nanocrystal Quantum Dots - J. Phys. Chem. B, 2002, 106 (31), pp 7619-7622

[9] X. Michalet, F. F. Pinaud, L. A. Bentolila, J. M. Tsay, S. Doose, J. J. Li, G. Sundaresan, A. M. Wu, S. S. Gambhir, S. Weiss - Quantum Dots for Live Cells, in Vivo Imaging, and Diagnostics - Science Vol. 307. no. 5709, pp. 538 - 544

[10] Ballou, B; Lagerholm, Bc; Ernst, La; Bruchez, Mp; Waggoner, As (Jan 2004). ”Noninvasive imaging of quantum dots in mice.” (Free full text). Bioconjugate chemistry 15 (1): 79-86

[11] Materials Research Society fall meeting. Shortfalls in electron production dim hopes for MEG solar cells.”. Science (New York, N.Y.) 322 (5909): 1784

[12] L. J. Geerligs, V. F. Anderegg, C. A. van der Jeugd, J. Romijn, and J. E. Mooij, Europhysics Letters, 10(1):79-85, September 1989.

[13] SikorskiCh and Merkt U 1989 Phys.Rev.Lett. 62 2164

[14] Meurer B, Heitmann D and Ploog K 1992 Phys. Rev.Lett. 68 1371.

[15] Ashoori R C , Stormer H L, Weiner J S, Pfeiffer L N, Pearton S J, Balswin K W and West K W 1992 Phys. Rev. Lett. 68 3088.

[16] Drexler H, LeonardD, Hansen W, Kotthaus J P and Pettroff P M 1994 Phys. Rev.Lett. 73 2252.

[17] F. M. Peeters Phys. Rev. B 42, 1486

[18] Kohn W 1961 Phys. Rev. 123 1242.

[19] Maxym P A and Chakraborty T 1990 Phys. Rev. Lett. 65 108.38

[20] Gu S W and Guo K X 1993 Solid State Commun. 89 1023.

[21] Johnson N F and Payne M C 1991 Phys. Rev. Lett. 67 1157.

[22] Johnson N F and Payne F C 1992 Phys. Rev. B 45 3819.

[23] Egger R, Hausler W, Mark C H and Grabert H 1999 Phys. Rev. Lett. 82 3320.

[24] Zhu K D and Gu S W 1993 Phys. Rev. B 47 12947.

[25] Zhu K D and Kobayashi T 1995 Solid State Commun. 95 805.

[26] Chen C Y, Jin P W , Lin D L 1997 Phys. Rev. 56 14913.

[27] Mukhopadhyay S and Chatterjee A 1998 Phys. Lett. A 242 355.

[28] Mukhopadhyay S and Chatterjee A 1995 Phys. Lett. A 204 411.

[29] Mukhopadhyay S and Chatterjee A 1996 Int. J. Mod. Phys. 10 2781.

[30] Mukhopadhyay S and ChatterjeeA 1997 Phys. Rev. B 55 9297.

[31] Mukhopadhyay S and Chatterjee A 1998 Phys.Rev. B 58 2088.

[32] Mukhopadhyay S and ChatterjeeA 1998 Phys. Lett. A 240 100.

[33] Mukhopadhyay S and Chatterjee A 1999 Phys. Rev. B 59 R 7833.

[34] Mukhopadhyay S and Chatterjee A 1999 J. Phys.: Condens.Matter 11 2071.

[35] Mukhopadhyay S and Chatterjee A 2000 Int. J. Mod. Phys. B 14 3897.

[36] Mukhopadhyay S and Chatterjee A 2002 Int. J. Mod. Phys. B 16 1489.

[37] Kervan N , Altanhan T and Chatterjee A 2003 Phys. Let. A 315 280.

[38] Krishna P M and Chatterjee A 2005 Physica B 358 191.

[39] Krishna P M and Chatterjee A 2005 Physica E 30 64.

[40] Krishna P M, Mukhopadhyay S and Chatterjee A 2006 Solid State Communn. 138 285.

[41] Sikorski Ch and Merkt U 1989 Phys. Rev. Lett. 62 21647.

[42] Demel T, Heitmann D, Grambow P and Ploog K 1990 Phys. Rev. Lett. 64 78891

[43] Meurer B, Heitmann D and Ploog K 1992 Phys. Rev. Lett. 68 13714.

[44] Ashoori R C, St rmer H L, Weiner J S, Pfeiffer L N, Baldwin K W and West K W 1993 Phys. Rev. Lett. 71

[45] Merkt U, Huser J and Wagner M 1991 Phys. Rev. B 43 73203